Review

Phosphates on Mars and Their Importance as Igneous, Aqueous, and Astrobiological Indicators

E. M. Hausrath [1,*], C. T. Adcock [1,†], J. A. Berger [2], L. M. Cycil [1], T. V. Kizovski [3], F. M. McCubbin [4], M. E. Schmidt [3], V. M. Tu [2], S. J. VanBommel [5], A. H. Treiman [6] and B. C. Clark [7]

[1] Department of Geoscience, University of Nevada, Las Vegas, NV 89154, USA
[2] Jacobs JETSII, NASA Johnson Space Center, Houston, TX 77058, USA; valerie.m.tu@nasa.gov (V.M.T.)
[3] Department of Earth Sciences, Brock University, St. Catharines, ON L2S 3A1, Canada
[4] NASA Johnson Space Center, Houston, TX 77058, USA
[5] Department of Earth and Planetary Sciences, Washington University in St. Louis, St. Louis, MO 63130, USA
[6] Lunar and Planetary Institute, Universities Space Research Association, Houston, TX 77058, USA; treiman@lpi.usra.edu
[7] Space Science Institute, Boulder, CO 80301, USA
* Correspondence: elisabeth.hausrath@unlv.edu
† Current address: School of Science, Engineering & Mathematics, College of Southern Nevada, 6375 West Charleston Blvd., Las Vegas, NV 89146, USA.

Abstract: This paper reviews the phosphate phases in meteorites and those measured by landed spacecraft, what they reveal about past igneous and aqueous conditions on Mars, and important implications for potential prebiotic chemistry, past habitability, and potential biosignatures that could be detected in samples returned from Mars. A review of the 378 martian meteorites as of 2023 indicate that of the two most common phosphate minerals in Mars meteorites, merrillite and apatites, the apatite composition is largely F- and Cl-rich, with shergottites containing more OH. The phosphate concentrations examined across multiple missions show a relatively narrow range of phosphate, with higher concentrations observed in the Mount Sharp Group in Gale crater and Wishstone at Gusev crater and lower concentrations observed at Jezero crater floor and Jezero fan. Possible secondary phosphates detected on Mars, including Fe phosphates at Jezero crater and Gusev crater and Ca- and Al-bearing secondary phosphates, temperatures of formation of secondary phases and their dissolution rates and solubilities are reviewed and summarized. Despite this wealth of information about phosphates on Mars, due to their fine scale and relatively low concentrations, Mars Sample Return is needed to better understand phosphate and its implications for the igneous, aqueous, and astrobiological history of Mars.

Keywords: phosphate; Mars; astrobiology; habitability; biosignatures; Mars Sample Return

1. Introduction

Phosphate is an essential chemical component of life on Earth, used in ATP for energy storage, in DNA and RNA for the structure of heredity transmission, and in phospholipid membranes for enclosing cells and their organelles [1]. Phosphate is also suggested to be essential in the prebiotic formation of RNA on Earth [2] and is the most common limiting nutrient on Earth [3–6]. Phosphate can be used as an important indicator of past life on Earth, with phosphate depletion both acting as a biosignature in paleosols [7,8] as well as phosphate minerals encrusting microbial cells [9–11]. Phosphates have been previously suggested as important targets for sample collection on Mars [12,13], and in the astrobiological study of Mars, examination of phosphate is therefore critical.

Increasing the importance of phosphate to the study of Mars, Mars is approximately 8 times richer in phosphate than Earth [14,15]. Igneous phosphate-bearing minerals including apatite [16], chlorapatite [17–19], and merrillite [18,19] are present in Mars meteorites

and provide critical information about past volatile conditions, melt evolution, and crystallization on that planet [20–29]. As an incompatible element, phosphorus is variably enriched in martian magmas by igneous processes [30], and igneous phosphates commonly occur among late-stage crystalline assemblages. Igneous phosphates therefore can provide important information regarding the igneous history of Mars.

Phosphate minerals can also be indicators of previous aqueous activity on Mars [31–34]. Little phosphorus enters the gas phase at the conditions of the martian surface and atmosphere [5], so its distribution near the martian surface reflects interactions between rock and aqueous fluids. These interactions vary according to temperature, pH, oxidation state (Eh), water chemistry, water–rock ratio, and time. Phosphate from solution can form crystalline phosphate minerals (mostly hydrated), substitute as a trace structural component into other minerals, be incorporated into amorphous materials, and be adsorbed onto mineral surfaces. Each of these phosphate-containing products has the potential to preserve the physical and chemical conditions under which they formed. Hundreds of phosphate minerals have been found and described on Earth [35], the vast majority of which form in very specific geologic environments or settings, making these secondary minerals excellent indicators of formation conditions. Thus, similar to the way in which igneous minerals can serve as important indicators of mantle or magma volatiles and melt evolution, the aqueous alteration of igneous phosphate minerals is a critical recorder of past aqueous conditions on Mars.

The many spacecraft missions to Mars have now provided data allowing for the detection and inference of multiple phosphate minerals on the martian surface (Table 1). The *Sojourner* rover on *Mars Pathfinder* provided the first detections of phosphorus on Mars [36,37]. The subsequent MER rovers *Spirit* and *Opportunity* detected phosphorus in widely varying abundances in Gusev crater and Meridiani Planum, respectively [38–40] Instruments on the Mars Science Laboratory (MSL) rover *Curiosity* have provided both phosphorus abundances and X-ray diffraction detections of phosphate minerals in Gale crater [41–45]. With the landing of the Mars 2020 *Perseverance* rover in Jezero crater, microscale chemical, textural, and inferred mineralogical data are available for the first time for phosphate minerals on Mars. *Perseverance*'s samples, collected and cached for potential return to Earth [46–48], will provide unprecedented new information about phosphate phases on Mars.

Table 1. A summary of phosphate minerals that have been detected or inferred on Mars.

Name	Formula	Type [a]	Basis [b]	Ref.	Bio Ref.
Anapaite	$Ca_2Fe(PO_4)_2 \cdot 4H_2O$	S	Met	[49]	
Brushite	$CaPO_3(OH) \cdot 2H_2O$	S	Inf	[50,51]	[52–54]
Chlorapatite	$Ca_5(PO_4)_3Cl$	I	Met	[19,50,55,56]	[57]
Collinsite	$Ca_2(Mg,Fe)(PO_4)_2 \cdot 2H_2O$	S	Met	[49]	
Ferristrunzite	$Fe^{3+}Fe^{3+}_2(PO_4)_2(OH)_3 \cdot 5H_2O$	S	Inf	[58]	
Fluorapatite	$Ca_5(PO_4)_3F$	I,M,S	Met/ Mars	[41,42,59–64]	[65,66]
Giniite	$Fe^{2+}Fe^{3+}_4(PO_4)_3(OH)_5 \cdot 2H_2O$	S	Inf	[58,67–69]	[70]
hydroxyapatite	$Ca_{10}(PO_4)_6(OH)_2$	I,M,S	Met	[64,71]	[72,73]
Holtedahlite	$Mg_2(PO_4)(OH)$	S	Met	[49,74]	
Jahnsite group	$(Ca,Mn,Na)(Fe,Mn,Mg)(Fe,Mn,Mg)_2(Fe^{3+})_2(PO_4)_4(OH)_3 \cdot 8H_2O$	S	Inf	[75–77]	

Table 1. *Cont.*

Name	Formula	Type [a]	Basis [b]	Ref.	Bio Ref.
Keplerite	$Ca_9(Ca_{0.5}\square_{0.5})Mg(PO_4)_7$	I,M-Sh	Met	[78,79]	
Laueite	$Mn^{2+}Fe^{3+}_2(PO_4)_2(OH)_2 \cdot 8H_2O$	S	Inf	[44]	
Merrillite	$Ca_9(Na,Mg)(PO_4)_7$	I,M-Sh	Met	[19,39,50,55,80]	[31,74,81]
Metavivianite	$Fe^{2+}Fe^{3+}_2(PO_4)_2(OH)_2 \cdot 6H_2O$	S	Inf	[34]	
Monetite	$Ca(HPO_4)$	S	Inf	[50]	[81,82]
Monazite	$REE(PO_4)$	I	Met	[56]	
Strengite	$FePO_4 \cdot 2H_2O$	S	Inf	[58]	
Strunzite	$Mn^{2+}Fe^{3+}_2(PO_4)_2(OH)_2 \cdot 6H_2O$	S	Inf	[44]	
Tuite	$\gamma\text{-}Ca_3(PO_4)_2$	M-Sh	Met	[83,84]	
Variscite	$AlPO_4 \cdot 2(H_2O)$	S	Inf	[85,86]	[87]
Vivianite	$Fe_3(PO_4)_2 \cdot 8H_2O$	S	Inf	[34,88,89]	[90]
Whitlockite	$Ca_9(Fe,Mg)HPO_4(PO_4)_6$	S, I	Inf	[50,80]	[91]
Xenotime	$REE(PO_4)$	I	Met	[92,93]	

NOTE: $\square$ = site vacancy. a. For Type, I = igneous and/or primary; S = secondary mineral; M = metamorphosed or metasomatic; M-Sh = shock-metamorphosed/altered mineral. b. Basis of relevance to Mars, where Met = observed in martian meteorites, Mars = identified on Mars, Inf = inferred or theorized on the basis of direct Mars measurement, Mars meteorites, or Mars-relevant experimental data. For a more specific basis of Mars detection and biological occurrences, please see Table S1.

Thus, a comprehensive review of Mars' phosphorus distribution and phosphate mineralogy is timely in helping understand the planet's astrobiological potential, aqueous history, and phosphorus cycle and availability. In this review, we examine five aspects of phosphate on Mars: (i) Igneous phosphates; (ii) summaries of phosphate observations from the MER and MSL and (iii) Mars2020 rovers; (iv) phosphates as aqueous indicators, including leaching, sorption, and formation of secondary phases; and (v) the astrobiological implications of phosphate, including its implications for Mars Sample Return.

2. Meteorite Summary and Mineral Assemblages

Meteorites from Mars were first identified in the early and mid-1980s, e.g., [94]. By the mid-1990s, nearly a dozen meteorites had been confirmed as martian [95,96]. As of the end of 2023, over 378 martian meteorites have been identified [97]. They are principally recognized as martian based on the identification of trapped martian atmospheric gasses in shock-melted glasses, as well as multiple additional lines of evidence, including their oxygen isotopic compositions, the Fe/Mn ratios in mafic minerals, REE fractionations, and their late crystallization ages, all consistent with their origin from a large, recently active planetary body [94,98–100]. All but one martian meteorite are mafic to ultramafic igneous rocks and are broadly classified into five main groups, including shergottites (basalts, gabbros, and diabases), nakhlites (clinopyroxenites), chassignites (dunites), and orthopyroxenite Allan Hills (ALH) 84001 [99,100]. The fifth group comprises the regolith breccia meteorite Northwest Africa (NWA) 7034 and its pairs, which are composed mostly of basaltic fragments [99–102]. Like all meteorites, the martian meteorites have each experienced various amounts of shock and shock alteration from the impacts that eventually delivered them to Earth. Nonetheless, at this time, these meteorites represent the only martian samples here on Earth.

Phosphate minerals are described as minor minerals (<10% vol.) in martian meteorites but are ubiquitous across all known samples [25,27,29,64]. Merrillite and apatite are by far the most common phosphates; they are igneous in origin and typically occur as minor, late-stage phases included in, or interstitial to, mesostasis, feldspar, or maskelynite (shock-produced feldspar glass) (Figure 1) [25,27,29]. In rare occurrences, the high-pressure

phosphate mineral tuite (γ-$Ca_3(PO_4)_2$) has been identified in highly shocked martian meteorites associated with impact-produced melt pockets and veins (i.e., [83,84]. Finally, rare grains of monazite and several other REE phosphates have been discovered as inclusions in apatite in the basaltic regolith breccia meteorites [92].
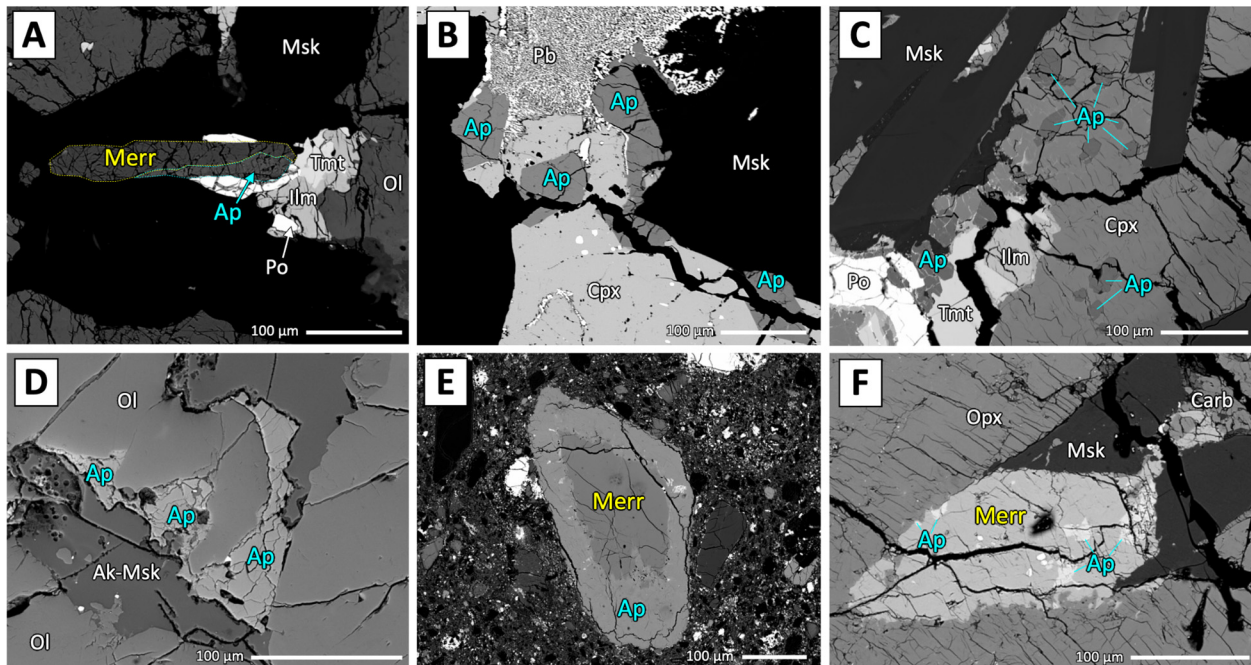
Figure 1. Backscattered electron images of apatite and merrillite in martian meteorites. (**A**) Intergrown merrillite (Merr) and apatite (Ap) associated with maskelynite (Msk) and late-stage minerals, including ilmenite (Ilm), titanomagnetite (Tmt), and pyrrhotite (Po) in shergottite RBT 04261 (adapted from [25]). (**B**) Subhedral apatite (Ap) associated with clinopyroxene (Cpx), maskelynite (Msk), and late-stage pyroxferroite breakdown products (Pb) in shergottite Los Angeles (adapted from [25]). (**C**) Apatite (Ap) inclusions in Ca-rich clinopyroxene rims in shergottite Shergotty (adapted from [25]). (**D**) Anhedral apatite (Ap) associated with alkali-rich maskelynite (Ak-msk) and olivine (Ol) in chassignite NWA 2737 (adapted from [27]). (**E**) Apatite (Ap) rimming merrillite (Merr) in the matrix of regolith breccia NWA 7034 (adapted from [29]). (**F**) Anhedral merrillite (Merr) intergrown with carbonate (Carb) and apatite (Ap) in orthopyroxenite ALH 84001 (Opx = orthopyroxene) (adapted from [20]).

2.1. Merrillite

Merrillite is the most common phosphate mineral in martian meteorites and is 2–3$\times$ more abundant than apatite in depleted shergottites [19,25,29,31,80]. Merrillite is a volatile-free phosphate ($Ca_9Na[Fe,Mg][PO_4]_7$), technically classified as ferromerrillite when Fe > Mg (ideal end-member formula $Ca_9NaFe[PO_4]_7$; [103]), and forms a solid solution with the H-bearing phosphate mineral whitlockite on Earth ($Ca_9[Fe,Mg][HPO_4][PO_4]_6$) [104]. Whitlockite has not yet been identified on Mars, in martian meteorites, or in any extraterrestrial material to date (although in the past, merrillite was commonly incorrectly identified as whitlockite in meteorites, before differences in the H contents and crystal structures between the two minerals were discovered [104–107]). While merrillite is the dominant phosphate phase in depleted shergottites and the orthopyroxenite ALH 84001, it is generally considered an extraterrestrial mineral, and it has only been identified on Earth within mantle xenoliths from Siberia, Russia [108], potentially as inclusions in lower-mantle diamond [109], or as a minor solid solution with whitlockite [104,110]. In contrast to the primary nature of merrillite and its prevalence in extraterrestrial and martian materials, whitlockite is rare on Earth and is generally found as a hydrothermal phase in association with pegmatites or as a biomineral in bones [104,111].

While merrillite is generally abundant across the shergottite martian meteorites and in ALH 84001, it is absent in nakhlites and chassignites (which only contain apatite) and is only rarely observed in the polymict breccias when intergrown with or rimmed by apatite [25,27,29]. Where present in shergottites and ALH 84001, merrillite can be observed in a variety of textural occurrences and is typically associated with late-stage minerals and mesostasis [18,25,26,29]. It is also commonly intergrown with apatite, rimmed by apatite, or contains apatite inclusions. In orthopyroxenite ALH 84001, igneous merrillites are observed in close association with secondary carbonates [18]. Merrillite in martian meteorites ranges in size from 10 μm up to several hundreds of μm, occurring in a variety of forms, from euhedral pseudo-hexagonal crystals to irregular anhedral shapes [18,25,26,29].

2.2. Apatite

Apatite ($Ca_5(PO_4)_3$(Cl, F, OH)) is a minor phase in the majority of martian meteorites and can be observed in a variety of textural occurrences. Martian apatites are generally enriched in Cl in comparison to igneous apatites on Earth [22]. Their volatile compositions can vary significantly within a single meteorite, but some broad compositional trends in OH, F, and Cl can be used to distinguish between apatites within various martian meteorite groups (Figure 2). Apatites within shergottites show the most variability in OH, F, and Cl; apatites in the polymict breccias are notably rich in Cl; and apatites within the nakhlites and chassignites contain little OH and variable F:Cl compositions [18,20,25,27,28,112]. The apatite in orthopyroxenite ALH 84001 exhibits substantial variability in its F, Cl, and OH abundances on a grain–grain basis in the sample [20].

In shergottites, apatite commonly occurs as discrete grains and/or intergrowths, with merrillite associated with typical late-stage phases like Fe-oxides, sulfides, K-rich feldspar, etc., located within mesostasis material [25,29]. More rarely, subhedral to euhedral apatites are present as inclusions within Ca-rich pyroxene rims (in the Shergotty meteorite) or as small (<10 μm) patchy anhedral growths on the rims of merrillite and pyroxenes (possibly formed through rock–fluid interactions) [25]. While precise modal abundance estimates for apatite minerals in shergottites are not widely available, it is generally known that apatite typically occurs in higher abundances in incompatible trace element (ITE)-enriched shergottites relative to ITE-depleted shergottites [25]. In the chassignites, apatite is present in their intercumulus mesostases and within olivine-hosted melt inclusions [16,27,28]. The apatite grain sizes and shapes vary significantly within the chassignites (<1 to 40 μm in the shortest dimensions and grain shapes from euhedral to anhedral [16,27,28]).

In the nakhlites, three main populations of apatite have been identified based on their textural associations and chemical compositions, including (i) apatites associated with maskelynite and titanomagnetite (sometimes as discrete inclusions within titano-magnetites), with high Cl concentrations and limited F:Cl ratio variability; (ii) apatites associated with late-stage mesostasis material, as equant grains with highly variable F:Cl ratios; and (iii) highly acicular F-rich apatites occurring within mesostasis with limited F:Cl ratios [21,27]. These three apatite populations in the nakhlites are thought to have resulted from the crystallization of Cl-rich magmas that reached saturation in a Cl-rich fluid that was lost during ascent and/or eruption [21,27].

In the polymict regolith breccia meteorites, apatite is found within the majority of the polymineralic clasts and as discrete grains throughout the matrix [113,114]. The largest apatite grains (~100 s of μm) occur as anhedral grains in the coarser-grained igneous clasts associated with orthoclase, plagioclase, and ilmenite (known as monzonite or Fe-Ti-P-rich (FTP) clasts; [102,114]). Although apatite exists in multiple textural domains within the polymict regolith breccia, they are all rich in Cl and exhibit somewhat limited variability in their F:Cl:OH ratios (Figure 2). Moreover, the ages of the apatite grains are all within uncertainty of ~1.5 Ga [113,115]. In fact, apatite yielding an age of 1.5 Ga coexists in an igneous lithic clast that hosts zircons that exhibit an age of ~4.4 Ga [113]. These three observations all support the hypothesis that the polymict regolith breccia underwent

hydrothermal alteration by Cl-rich crustal fluids at ~1.5 Ga that reset some of the mineral chronometers and altered the volatile abundances of apatite [20,92,113,115].

2.3. Tuite

The high-pressure phosphate mineral tuite is found in highly shocked martian meteorites [83,84]. It typically occurs as minute grains (~1–3 μm in size) associated with impact melt glasses and shock veins [83,84]. Tuite can form after either apatite or merrillite is subjected to high-pressure and temperature impact events and has been synthesized at 12–15 GPa and 1100–2300 °C [116,117]. As such, the presence of tuite in meteorites can be used to constrain the pressure and temperature conditions the sample has experienced during impact events.

REE Phosphates

Rare REE-rich phosphate phases, including monazite ([LREE]PO_4) and xenotime (YPO_4), have been observed in the martian regolith breccia meteorites (NWA 7034 and pairs; [92]). Monazite has been observed in the breccias as clusters of minute inclusions within isolated apatite grains (Ce-monazite) and as sub-micrometer crystals (Ce,Nd-monazite) intergrown with REE-rich silicates in a trachyandesite clast [92]. Xenotime has been reported in a unique occurrence, associated with alteration materials in a unique pyrite–ilmenite–zircon-bearing clast [92]. The zircon in this clast is hydrothermally altered, and as such, alteration is inferred to be the most likely source of Y and HREE to form xenotime [92].
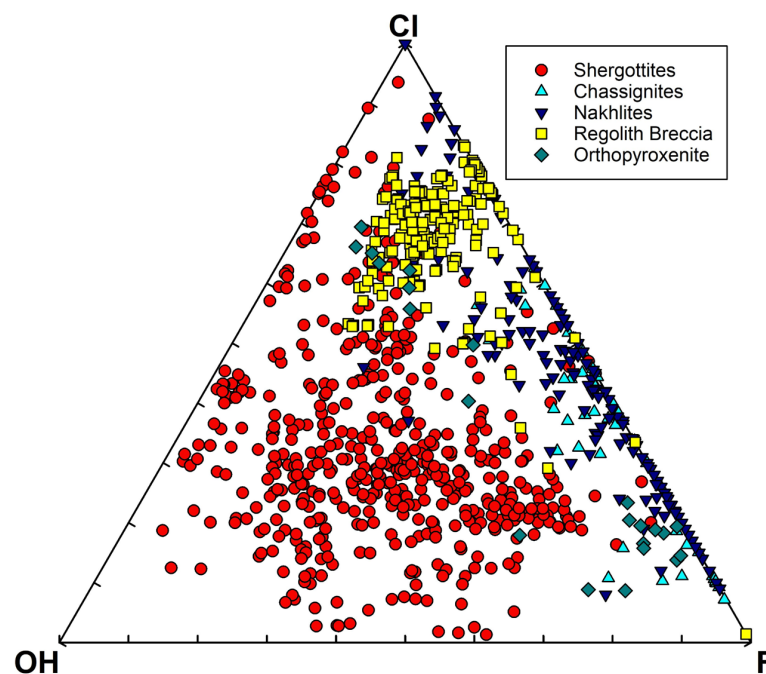
Figure 2. Ternary plot of apatite X-site components (mol%) from all martian meteorite types from the literature, including shergottites [24,25,112,118–125], chassignites [16,27,28,126], nakhlites [21,27,127], regolith breccia [25,92,113–115,128], and cumulate orthopyroxenite [20,129]. The OH component was calculated based on 1 − F − Cl = OH. All data plotted in the ternary are tabulated in Table S2.

3. Phosphate Detections and Analyses from Spacecraft Missions

3.1. Early Missions

***Viking*:** The Viking lander reported chemical compositions but did not report P concentrations because they were not detectable by the XRF instrument [130–133]. ***Pathfinder*:** The first chemical results from Pathfinder [37] did not report phosphorus concentrations. Recalibrated data using a laboratory spare instrument in a Mars-like chamber gave P con-

centrations that ranged from 0.4 to 0.7 weight percent for rocks and from 0.3 to 1.2 weight percent for soils [134,135]. ***Phoenix***: Chemical analysis capabilities of the Phoenix mission were dominantly in its Wet Chemistry Laboratory (WCL), which was designed to detect common water-soluble cations and anions, including the cations K^+, Na^+, NH_4^+, Ca^{2+}, and Mg^{2+} and the anions Cl^-, Br^-, I^-, NO_3^-/ClO_4^-, and SO_4^{2-} [136]. The WCL could not detect phosphate.

3.2. Spirit

The Mars Exploration Rover (MER) Alpha Particle X-ray Spectrometer (APXS) generated the first P concentrations for martian rocks and soils in situ during the mission timeline. In Gusev crater, the rover *Spirit's* APXS found high concentrations of P (~5 wt.% P_2O_5) with low Cr (below detection) in Wishstone-class rocks (i.e., Wishstone and Champagne) [38,39,51]. Watchtower rock has been suggested to be related to the Wishstone-class rocks, perhaps as a product of aqueous alteration [51,137]. Post-grind analyses of both Watchtower and Wishstone resulted in an increase in both P_2O_5 and CaO compared to pre-grind [50,51,137,138]. To explain this observation, it has been proposed that a phosphate mineral might have been lost from the surface due to dissolution [50,55]. Lacking direct mineralogical data, several phases are possible. Hurowitz et al. [137] suggested merrillite, monetite, or brushite; Ming et al. [51] proposed apatite, brushite, or strengite, an Fe phosphate phase; Adcock and Hausrath's [55] reactive transport modeling results are consistent with the presence of multiple Ca phosphate minerals in Wishstone-class rocks (i.e., merrillite and apatite); and Ruff et al. [139] suggested wavellite, an Al phosphate phase, for Watchtower.

Ferric iron phosphate minerals have been proposed for several *Spirit* targets. For the extensively hydrothermally altered, sulfate-rich soil of the Paso Robles target, the suggested phosphate minerals include strengite, ferristrunzite, and ferrian giniite [58,140].

3.3. Opportunity

Rocks at Meridiani Planum contain abundant P [141], which has been attributed to the presence of soluble phosphates [40]. Localized phosphate enrichment of up to 2.44% is also associated with high Mn and S levels at Endeavor crater, suggesting mobility in sulfate-rich fluids [142]. More recently, examination of the P levels and P:Ti ratios indicate that they are similar to the levels and ratios in martian basalts, which has been interpreted as immobilization of the phosphate in secondary Fe and Al phosphate phases, such as the Fe phosphate ferrian giniite [69]. Additionally, Pinnacle Island exhibited high Mn and P contents in the APXS target "Jelly Donut", associated with alteration coatings [142].

3.4. Curiosity

Since landing on 5 August 2012, the Mars Science Laboratory (MSL) rover *Curiosity* has been exploring rocks in Gale crater, including the layered sedimentary units making up Aeolis Mons (informally known as Mount Sharp) at its center. The Chemistry and Mineralogy Instrument (CheMin) X-ray diffractometer provides direct detections of phosphate minerals, and chemical analyses by both APXS and ChemCam LIBS provide evidence for phosphate-containing minerals and amorphous material.

Fluorapatite is present in many Gale crater rocks, directly detected by CheMin and indirectly by chemical analyses. At the time of writing this paper, Curiosity has drilled and analyzed a total of 40 samples. As previously reported, 36 of the samples were analyzed by CheMin, and 10 contained fluorapatite at >~2% weight [42,143]. Several chemical analyses by ChemCam LIBS show detections and levels of F and Ca consistent with fluorapatite [144], and a few APXS analysis targets (Nova, Rucker, and Waternish) are sufficiently enriched in Ca and P to suggest the presence of apatite [143]. The preservation of fluorapatite through erosion, deposition, and diagenesis in Gale crater suggests that the local chemical environments were not highly acidic, nor moderately acidic for long durations [145,146].

The rocks in Gale crater contain significant proportions of X-ray-amorphous materials [147–150], which likely contain phosphorus. The samples analyzed by CheMin and APXS contain ~0.5–2.1 wt.% P_2O_5, even those with no detectable fluorapatite [151]. That phosphorus is likely contained in phases (including fluorapatite) at abundances below CheMin's detection limit and in amorphous materials [42,62,146].

The rocks of Gale crater experienced a wide range of diagenetic processes [152], and some of these involved significant mobility of phosphorus with iron, manganese, and/or magnesium [151,153]. Veinlets and coatings rich in P and Fe-Mn-Mg are present across much of Gale's sediments, including mostly mudstones and siltstones [41,153,154]. A unique example of Mn-Fe-Mg phosphate diagenesis is the Groken rock in the Knockfarril Hill member of the Murray Formation [44]. There, centimeter-scale dark diagenetic nodules are calculated to contain more than 18 wt.% P_2O_5, presumably as phosphate, charge-balanced by Mn, Fe, and Mg. No X-ray diffraction data on the nodules were acquired, but Treiman et al. [44] proposed that the nodules were originally manganoan vivianite, a ferrous phosphate, and their current bulk compositions reflect its alteration into laueite or strunzite, which are ferric manganous phosphates. Thermodynamic modeling suggests that the nodules now might be more oxidized still, as with a manganic oxide mineral (e.g., MnO_2) and strengite, a ferric phosphate [44,155]. Other secondary phosphate minerals proposed for martian rocks include Al phosphate sulfate minerals, based on field analog work and phosphate enrichment in sulfate minerals in Gale crater [156,157]. Berger et al. [151] also document relatively consistent P_2O_5 concentrations (0.88 ± 0.22 wt.%), as measured by *Curiosity's APXS*, in the basaltic Sheepbed member the Stimson formation (not including the altered haloes) and alkali-rich sedimentary units. The fluvio-lacustrine mudstone and sandstone of the Mt. Sharp group, a volatile-rich, altered basalt sedimentary sequence, is enriched in P_2O_5 (0.99 ± 0.28 wt.%) relative to martian basalt (~0.8 wt.%); the enrichment mechanism(s) is (are) not well constrained. Among the Gale bedrock targets, localized diagenetic features in the Murray and Carolyn Shoemaker formations, Stimson fracture haloes, and the Amboy and Kern Peak targets in the remarkable Garden City vein complex contain elevated phosphate [41,151,158,159]. Phosphate enrichment in the veins of the Stimson formation's sandstone is attributed to a potential Fe phosphate mineral [41] and/or sorption [160].

3.5. Mars 2020 PIXL

The Mars 2020 rover "*Perseverance*" landed on the floor of Jezero crater (an ancient impact crater with a ~45 km diameter that once contained a lake [161]) on 18 February 2021 and has since traversed over 20 km across the crater's floor and western fan. Throughout this mission, phosphate minerals in Jezero crater have been detected using several instruments, including SuperCam [162,163], SHERLOC [164] and PIXL [34,165–167]. The high-resolution chemical and textural data provided by PIXL are particularly useful in identifying and characterizing phosphate minerals, which typically form small, rare grains (i.e., Figure 1; [18,25,26,29]).

The Planetary Instrument for X-ray Lithochemistry (PIXL) is a scanning X-ray fluorescence (XRF) spectrometer which collects the elemental compositions of spots ~120 μm in diameter and typically is used to produce element abundance maps at that spatial resolution [168]. At the time of writing, Perseverance has analyzed over 25 outcrops with PIXL [167,169,170]. Phosphate minerals (defined as PIXL XRF analysis points with P_2O_5 >5 wt.%; [34,165,166]) have been identified in almost all targets to date.

In most rocks in which phosphates have been identified, the PIXL analyses show a positive correlation between the abundance of P_2O_5 and CaO, indicating that Ca phosphate minerals dominate the rocks' P budgets [167]. However, Fe phosphate grains were found in the Onahu conglomerate in Jezero crater's western fan [34]. The grains of phosphate minerals are typically smaller than PIXL's spot size (~120 μm), so phosphate mineral stoichiometry (e.g., Ca:P and Fe:P ratios) must be inferred from the chemical mixing trends between phosphates and the surrounding silicates [34,165–167].

Using the chemical and textural information collected by PIXL, the phosphate minerals across Jezero crater can be grouped into four main occurrences (Figure 3):

1. Igneous phosphate minerals observed within or interstitial to mesostasis/feldspar and adjacent to other late-stage phases such as Fe-Ti oxides [165,167]. The Ca:P (molar) ratios and mixing trends in the igneous rocks on the Jezero crater floor are consistent with apatite and merrillite. Merrillite is dominant in the olivine cumulate rocks of the Séítah formation [167], while the highly evolved basalts of the Maaz formation contain apatite and merrillite [165]. However, it should also be noted that merrillite and apatite are commonly intergrown in igneous martian meteorites at length scales below PIXL's spot size (i.e., [25,29]; Figure 1).

2. A phosphate phase with Ca:P (molar) = ~1 was detected in the igneous rocks of the crater floor, associated with altered olivine, Cl-rich alteration, and mesostasis [165]. Sediments of the Jezero fan also contain rare grains of this mineral. It is likely a secondary phase, possibly brushite [165,166].

3. Detrital phosphate minerals in the sedimentary rocks of the Jezero fan. Stoichiometry (e.g., Ca:P ratios) from mixing trends are consistent with apatite and merrillite, suggesting that the grains might be from igneous source rocks [166].

4. Blue/green Fe phosphates have been identified in the conglomerate outcrop (Onahu) within the western fan of Jezero crater. These Fe phosphates have an Fe:P ratio and color consistent with those of vivianite ($Fe_3[PO_4] \cdot 2H_2O$; although the exact Fe phosphate phase is not certain at this time) and occur in the matrix surrounding clasts of Fe-Mg silicate minerals [34].
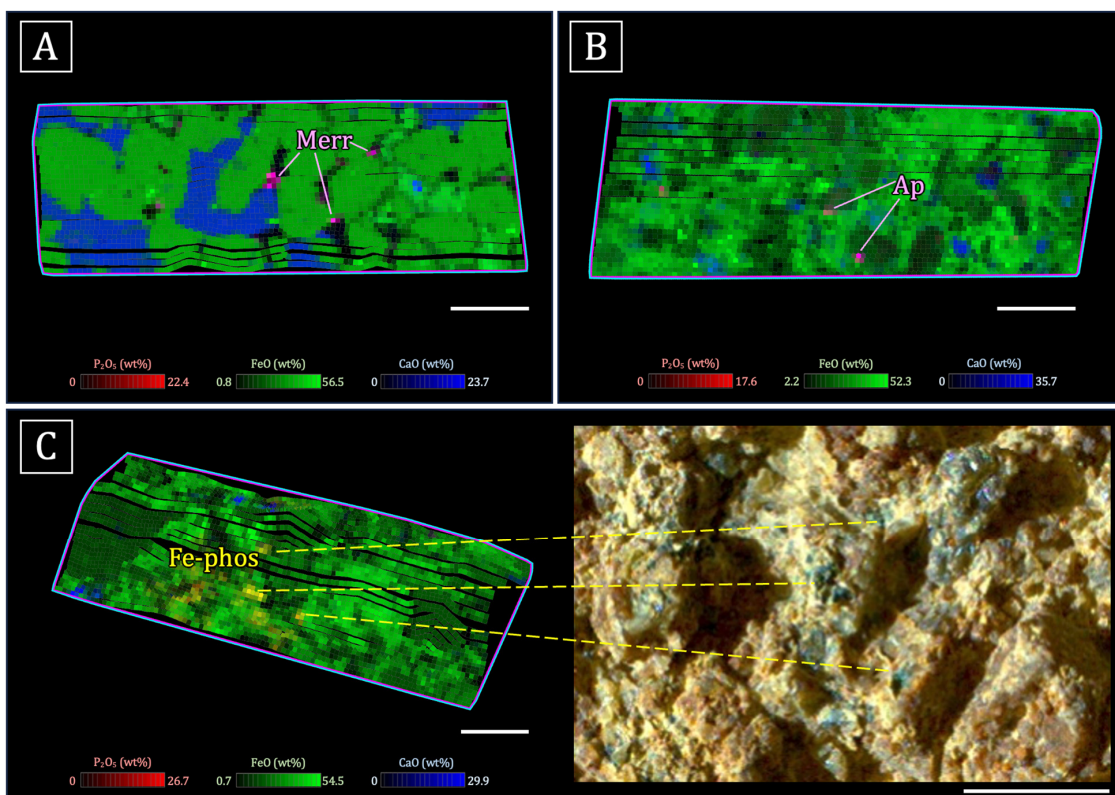
Figure 3. PIXL Red/Green/Blue (RGB) maps of P_2O_5, FeO, and CaO, respectively, highlighting occurrences of Ca phosphates in pink and Fe phosphates in yellow. White bars represent ~2 mm scale bars for each image. (**A**) Igneous merrillite in the Séítah abrasion patch Dourbes located within the mesostasis (meso) between cumulus olivine (Ol) and pyroxene (Px). (**B**) Detrital monomineralic apatite (Mono-Ap) in the Thornton Gap abrasion patch within the delta. (**C**) Fe phosphates in the Ouzel Falls abrasion patch within the Onahu conglomerate outcrop within the delta, and a close-up

of a WATSON image showing the blue/green color of the Fe phosphates (WATSON image: SI1_0789_0736995354_613FDR_N0390926SRLC000 36_000095J01.IMG, enhanced with 1% contrast stretch).

3.6. Global Observations from Mars Missions

Across multiple missions, the concentrations of phosphate are largely consistent (Figure 4). The highest concentrations plotted are in the Wishstone rocks of Gusev crater and the Mt. Sharp group rocks of Gale crater, although the Groken nodules have higher concentrations at 18%, which do not fill the APXS's field of view [44,45], and the lowest are from the Jezero fan and crater floor samples, but in general, the samples are confined within one order of magnitude of the martian crust (0.83 wt.%) [171] (Figure 4).
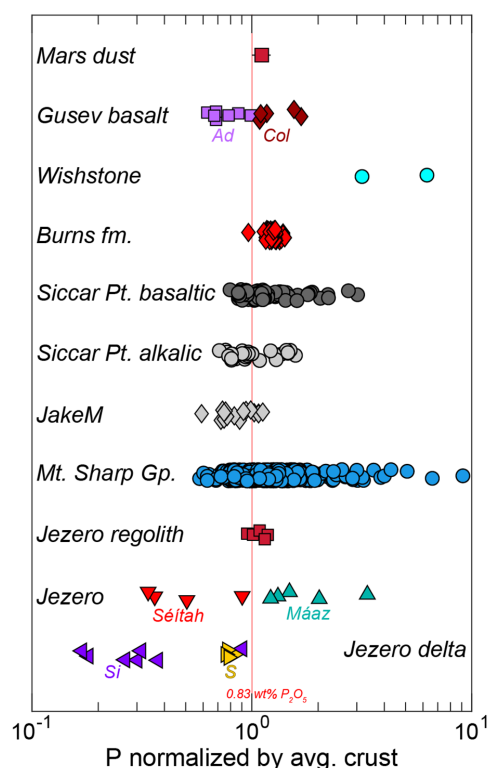
Figure 4. Comparison of in situ phosphorus measurements by four Mars rovers, normalized by the average P_2O_5 of the martian crust (0.83 wt.%) [171]. Mars dust P_2O_5 is estimated from MER measurements of bright soils [172]. Selected APXS results are shown from Spirit (Gusev basalt-Adirondack, Ad, and Columbia Hills alkali basalts, Col, Wishstone) [173], Opportunity (Burns formation) [69,174,175], and Curiosity (Siccar Point group, Jake, and Mt. Sharp group) [151,154,176–178]. Results from the PIXL instrument on Perseverance show phosphorus concentrations in Jezero crater (regolith, abraded rock of the Máaz and Séítah formations and the siliciclastic [Si] and sulfate [S] delta facies). Ca sulfate veins and nodules are omitted.

Observations across multiple missions also support the observation that dust is enriched in phosphate relative to soil [40,134,138,157,179–181]. The composition of the dust collected on the Mars Exploration Rover magnets indicate enrichment in P relative to the soil [179]. This is consistent with a number of measurements from Pathfinder and the Mars Exploration Rovers suggesting that soil on Mars is enriched in P relative to rock [40,134,138]. Positive correlations of P with S, Cl, and Zn in sand and soil, greater in soil than in sand, have been similarly interpreted as enhanced P concentrations in dust in Gale crater [157,180]. Measurements of the dust collected on the PIXL calibration target indicate that the dust is enriched in P relative to previous measurements of the soil from Gusev crater and dust and soil from Gale crater [181].

4. Phosphates as Aqueous Indicators

4.1. Dissolution of Phosphate Minerals

In terrestrial igneous rocks, fluorapatite is by far the most common primary phosphate mineral [182]. Phosphate minerals can reach substantial concentrations in some terrestrial igneous rocks like nelsonites and other associated FTP (Fe-Ti-P-rich) rocks [39,183–186], and in rare plutonic ultramafic rocks (i.e., phoscorites), they are essential rock-forming minerals [187]. However, most commonly, fluorapatite occurs as a minor accessory phase (<1% vol.).

Thermodynamic data indicate that calcium phosphate minerals (e.g., fluorapatite) are more soluble than iron, aluminum, and manganese phosphate minerals under acidic conditions (e.g., Figure 5). Similarly, their dissolution rates indicate that the dissolution of fluorapatite, chlorapatite, merrillite, and whitlockite is generally rapid relative to other phosphate minerals (Figure 6). Predictions from these laboratory data therefore suggest that Ca-bearing phosphate minerals would largely be dissolved and replaced by other pools of phosphate in water-containing environments. The behavior of phosphate in soils, described by the Walker and Syers model [6], is largely consistent with these predictions in humid environments [6,188–190]. Quantification in terrestrial chronosequences shows that Ca phosphate minerals persist in terrestrial tropical soils at the scale of <20,000 years [4]. Upon dissolution of the primary Ca-bearing phosphate minerals, the released phosphate is generally less mobile than the Ca [4], sorbing onto surfaces [191] or precipitating as secondary Al, Fe, or Mn phosphates [192].

However, in addition to the importance of time indicated in the Walker and Syers model, changes in phosphate behavior with lithology and climate are also important [193]. Examination of arid environments that may be more relevant to Mars indicate a much greater extent of apatite in arid soils versus humid soils [191], including the persistence of apatite in arid soils formed on basalts for millions of years [194] (Figure 7).
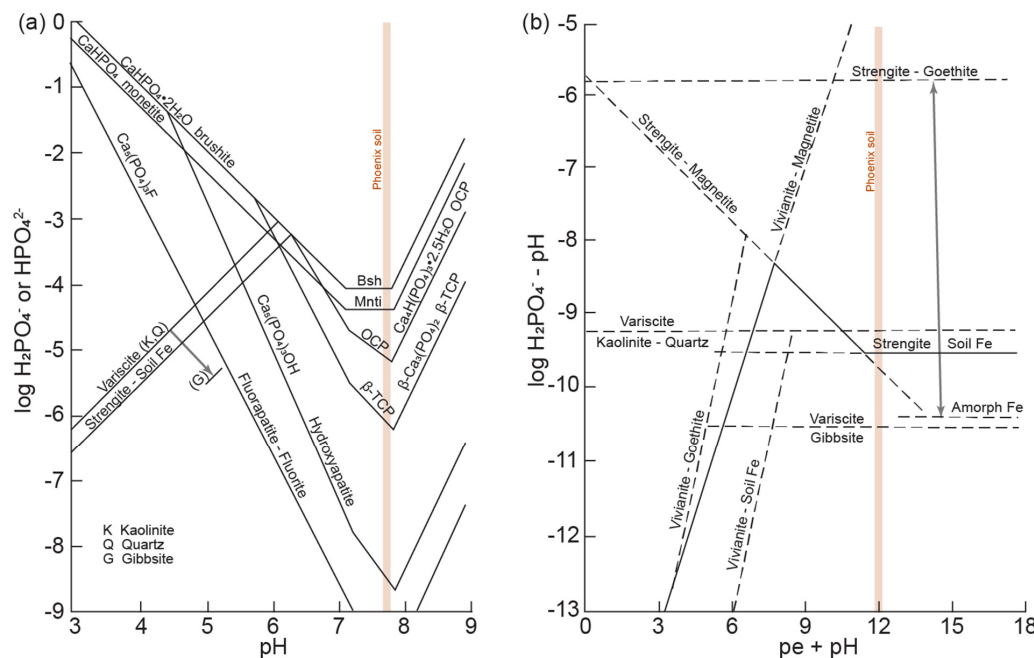
Figure 5. Solubilities of different P-containing minerals found in terrestrial soil environments, modified after Lindsay [195]. (**a**) The solubilities of Ca phosphates at 25 °C are shown compared to strengite and variscite when fixed by calcite and CO_2 at 0.0003 atm. (**b**) The effect of redox on the stability of Fe and Al phosphates is demonstrated by the redox conditions at 25 °C under which strengite, variscite, and vivianite are stable. The pe and pH of the Phoenix soil Rosy Red (4.3 and 7.7, respectively) are denoted for reference [196]; Phoenix did not measure PO_4^{3-} [136].
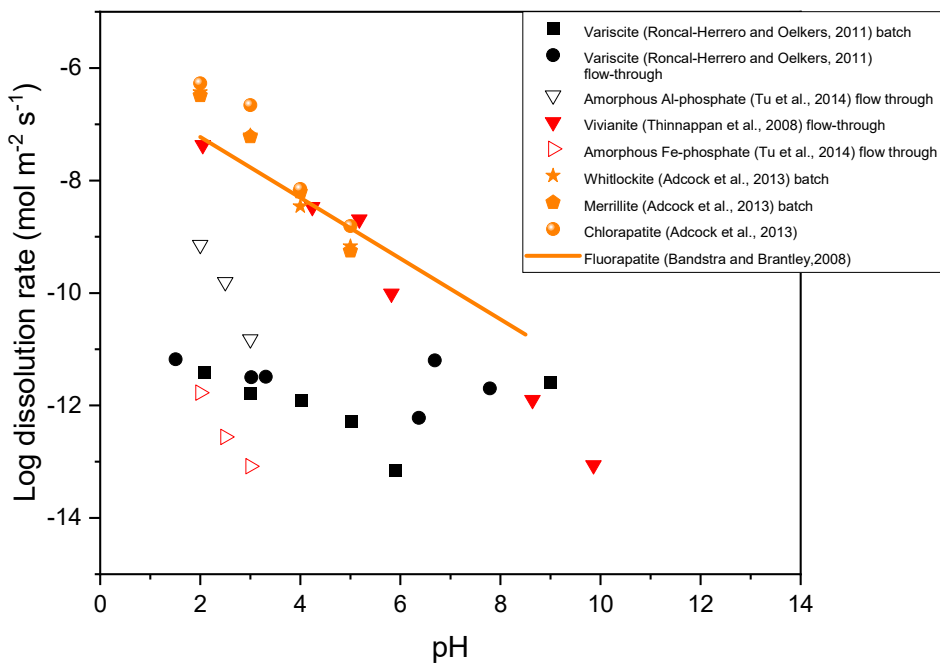
Figure 6. Dissolution rates of different phosphate-containing minerals plotted as a function of pH showing that Ca-bearing phosphates such as fluorapatite, whitlockite,merrillite and chlorapatite generally dissolve rapidly relative to other phosphates. Few data are available for Mn and ferric phosphates. Data compiled from [31,85,192,197–200] and presented in Table S3.
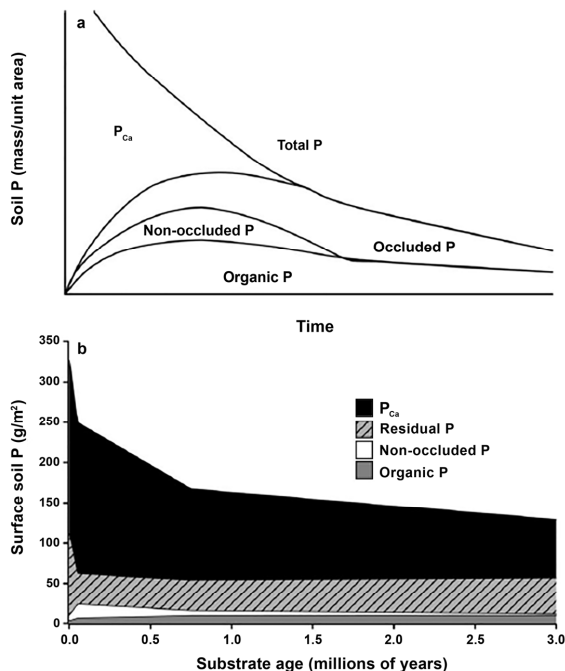

Figure 7. (**a**) Persistence of apatite in the classic Walker and Syers model [6] and (**b**) persistence of phosphate pools in a 3-million-year-old chronosequence formed on volcanic substrate under arid conditions [194]. Results show the persistence of phosphate in apatite for long periods of time in arid environments. Figure reproduced with permission from Selmants and Hart [194].

In general, under higher water:rock ratios, phosphate adsorbs, rather than precipitating as individual phosphate-containing phases (Figure 8) [201]. Phosphate anions chemisorbing onto nanophase Fe and Si/Al oxides in terrestrial soils affects the surface structure of the oxide particles [202] and may preclude mobility. Chemisorbed phases

are detectable by the Sample Analysis at Mars (SAM) instrument, as well as infrared spectrometers on landed missions [203].

$$M — OH_2^+ \text{-----} H_2PO_4^-$$ **Electrostatic attraction**

$$M — O — P \text{ (with OH, =O, OH)}$$ **Inner sphere monodentate surface complex**

$$M — OH_2^+ \text{-----} HPO_4^{2-}$$ **Electrostatic attraction**

$$M — O, M — O, P \text{ (with O, OH)}$$ **Inner sphere bidentate surface complex**
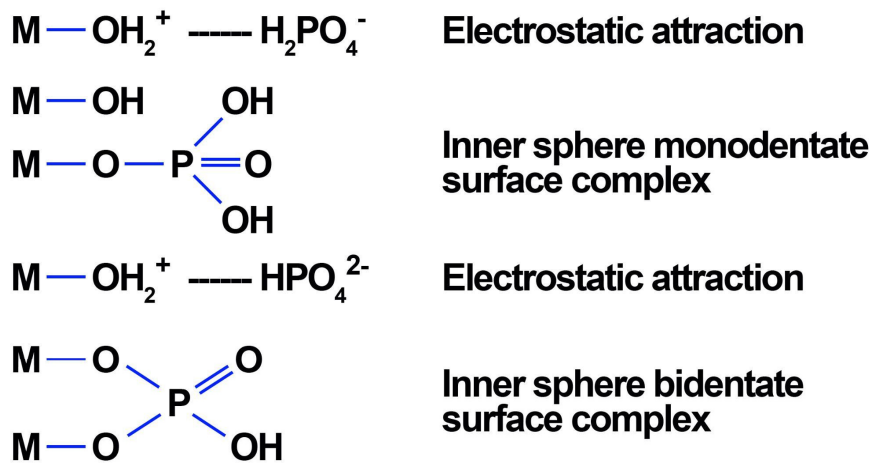
Figure 8. Figure showing the different types of adsorption of phosphate onto different surfaces. Figure is modified after Li et al. [204].

Under lower water:rock ratios than the higher water:rock ratios under which phosphate adsorbs onto mineral surfaces, distinct amorphous P-containing phases may precipitate [205]. Experiments indicate that these amorphous phases can then form crystalline phases, and that under even lower water:rock ratios, crystalline phases may precipitate [206,207]. Therefore, some have proposed that phases such as amorphous Al phosphates and variscite control the phosphate concentrations in natural environments on Earth [192]. Many phosphate minerals form solid solutions between ferric and Al phosphates [208], and Mars analog experiments have also generated Fe phosphate under acidic conditions [209], including ferrian giniite [140].

Under extremely low-water and acidic conditions, secondary calcium phosphate minerals such as monocalcium phosphate (MCP) and brushite form. In Mars analog acid vapor experiments, fluorapatite reacted with sulfuric acid vapor to form monocalcium phosphate monohydrate ($Ca(H_2PO_4)_2 \cdot H_2O$) (MCP) [140]. Monocalcium phosphate monohydrate is a common constituent of fertilizers used on Earth, and it forms brushite under common terrestrial soil conditions [210]. MCP would therefore, if found on Mars, be an indicator of low-water rock ratios. Brushite has also been reported to dissolve 3–4 orders of magnitude more rapidly than fluorapatite [211], and the presence of brushite would therefore also indicate extremely low-water rock conditions. Similar to secondary calcium phosphates such as MCP and brushite, Mg phosphates such as newberyite are very soluble, with their presence in meteorites [212] similarly indicating low-water conditions.

In addition, the oxidation state of the environment can impact the mobility of phosphate within aqueous environments when the phosphates contain redox-sensitive elements such as Fe or Mn (Figure 5). Previous studies have shown that manganese phosphates may be important in terrestrial soils [213]. Studies of multiple terrestrial soils have shown that solutions in many of the soils studied were oversaturated with respect to $MnPO_4 \cdot 1.5H_2O$ [213], and all of the Mn phosphates studied were more stable than the Fe and Al phosphates strengite and variscite under acidic conditions, with hureaulite and $MnPO_4 \cdot 1.5H_2O$ being the most stable [213]. Therefore, particularly due to the higher concentrations of Mn in martian basalts [214] than in terrestrial basalts [215], Mn-containing phosphates may be important indicators of past conditions on Mars.

4.2. Hydrothermal Phosphates as Temperature Indicators

Hydrothermal phosphates have been extensively studied in multiple settings on Earth [216–219], and it is known that different minerals form under different conditions,

including at different temperatures [218] (Figure 9) and depending on the pH, chemistry, and oxidation state of the reacting fluids [217,219]. This type of extremely valuable information about past hydrothermal environments may therefore be available for Mars if hydrothermal phosphates can be identified on Mars (e.g., [58]) or in returned samples.
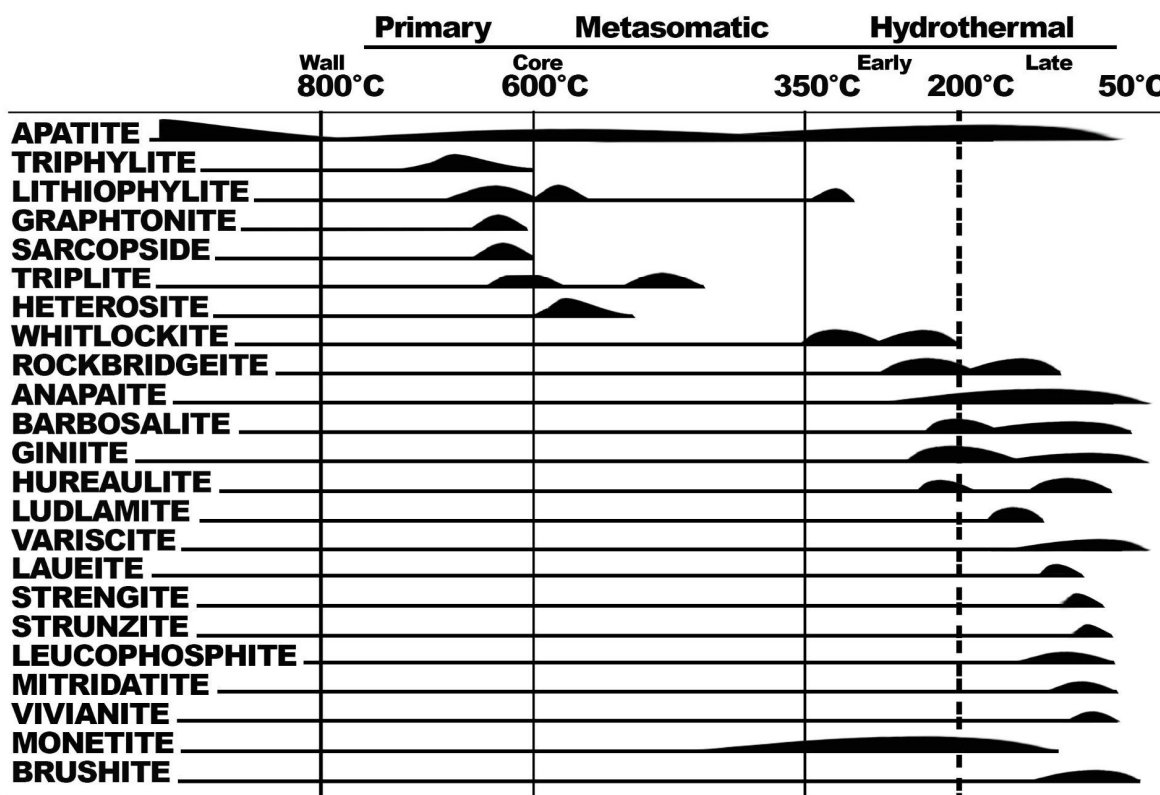

Figure 9. Approximate temperature ranges of formation/stability of different hydrothermal phosphates, modified after [218]. Lower-temperature phosphate minerals can also be biologically mediated (see Table 1). High P and T phases (e.g., holtedahlite, xenotime, tuite, merrillite) not included on diagram. Ranges are based on experimental work with both natural and synthetic phases, as well as paragenetic sequences.

4.3. Phosphates as Astrobiological Indicators

4.3.1. Habitability

Habitability has classically been defined as the intersection of sufficient liquid water; sufficient resources such as phosphorus, carbon, hydrogen, nitrogen, oxygen, and sulfur; sufficient energy; and sufficiently clement conditions, including factors such as temperature, salinity, and pH (Figure 10; [220,221]). Phosphate minerals can help interpret aspects of habitability (Figure 10). In long-term ecosystems, phosphate is the most common limiting nutrient [3,6], and therefore the presence of phosphate minerals indicates the presence of this critical, often limiting, nutrient. Igneous phosphate minerals dissolve rapidly in liquid water (e.g., Figure 6 [31], and the formation of secondary phosphate minerals can preserve evidence of the presence of liquid water, giving a record of this component that is essential to life as we know it. Finally, the characteristics of that liquid water that impact habitability, such as temperature and pH, can also be preserved in phosphate minerals (Figures 5 and 9 and Table 1).
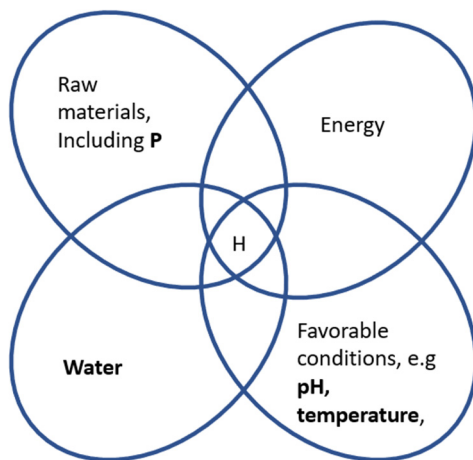
Figure 10. Classical interpretation of habitability (H) as the intersection of raw materials, water, energy, and sufficiently favorable conditions [220,221], with the aspects of habitability that phosphate minerals can directly help interpret (the presence of the most often-limiting nutrient P, water, pH, and temperature) shown in bold.

4.3.2. Prebiotic Chemistry

Phosphorus is also believed to be crucial to prebiotic chemistry. Phosphorus is present in phospholipids and has been found to form lipid bilayers in water similar in structure to cell membranes under prebiotic conditions [222–224]. Phosphate is present in RNA, which may have been both an early informational molecule for life, as well as a catalytic molecule in the proposed RNA world. Unlike other bioessential elements (C, H, N, O, and S), phosphorus does not have an abundant, naturally occurring gaseous phase [5]. The fundamental source of P for prebiotic chemistry must therefore arise from mineral weathering. Indeed, the difficulty of obtaining phosphorus has been considered to be so important to prebiotic chemistry that it might constrain prebiotic evolution. The "Phosphate Problem" has referred to the difficulty that low concentrations of phosphate in natural environments might pose for prebiotic chemical reactions [225]. Low concentrations of phosphate in natural environments on Earth result both from the relatively low solubilities of most phosphate-bearing minerals and the low concentrations of phosphate-bearing minerals in most rocks. To solve the "Phosphate Problem", some have suggested the importance of reduced phosphorus species released from iron-phosphide-bearing meteorites [226], as well as fulgurites [227], due to their enhanced solubility relative to phosphates. Studies have shown that reduced phosphides are fully oxidized into phosphates with the interaction of ultraviolet light [228]. Others have found that abiotic synthesis of RNA can occur with phosphate, which is used as general acid/base, and nucleophilic catalysts and a pH and chemical buffer [2]. Phosphate can become very concentrated in lakes with a high carbonate alkalinity [229].

4.3.3. Biological Mobilization of Phosphorus (P)

Soil microorganisms have a crucial role in the mobilization of phosphorus (P), both by mineralizing P from organic sources and solubilizing P from inorganic P pools. A specific subset of microorganisms, phosphate-solubilizing microorganisms (PSMs), can hydrolyze both organic and inorganic phosphate, including the production of phosphatase, an enzyme that releases bioavailable inorganic P from organic matter [230]).

Microorganisms can employ several mechanisms to access and solubilize P in soil, both from P-containing minerals (e.g., apatite) and to release P that is sorbed onto mineral surfaces. Key mechanisms are listed below:

(i)   Microorganisms can acidify their environment by releasing protons. Acidification is important because the dissolution of P-bearing minerals and processes such as desorption depend upon pH [231–233].

(ii) Microorganisms can release the anions of organic acids including citric, malic, malonic, oxalic, succinic, lactic, tartaric, gluconic, 2-ketogluconic, and glycolic acid [234,235]. Organic acids can increase the dissolution of P-bearing minerals by ligand-promoted dissolution and also cause the desorption of P from mineral surfaces by ligand exchange [232,236].

(iii) Microorganisms can release chelators such as exopolysaccharides and siderophores [232,237].

(iv) Microorganisms can physically attach to phosphate-containing minerals. In laboratory cultures, phosphate-limited cyanobacteria have been shown to preferentially attach to fluorapatite surfaces [238].

Laboratory experiments have demonstrated the effect of organic acids on phosphate-bearing whole rocks [7,239–241] as well as individual minerals in the presence of organic compounds [242–247] including the Mars-relevant Ca-phosphate-bearing minerals fluorapatite, merrillite, and whitlockite [248]. The dissolution of apatite-bearing rocks in the presence of organic compounds has shown enhancement of phosphate release in the presence of acetate, benzoate, citrate, formate, fumarate, gallate, glutarate, lactate, malonate, oxalate, phthalate, salicylate, and succinate [7,239–241]. The dissolution of fluorapatite in experiments containing organic compounds has indicated enhanced dissolution in the presence of acetate, citrate, oxalate, phthalate, and salicylate [243,246], and the dissolution of multiple Ca phosphate minerals relevant to Mars in experiments containing organic compounds relevant to Mars has indicated that the enhancement of dissolution by the organic compounds is likely due to the ligand denticity, the strength of the complex formed between the organic compound and calcium, and the saturation state of the solution [248]. The dissolution of hydroxyapatite in the presence of amino acids has indicated enhanced release of phosphate in the presence of aspartic acid but not alanine or lysine, which is attributed to the charge on the amino acids [244].

This preferential dissolution of phosphate-bearing minerals in the presence of organic compounds has been utilized as a signature of past life on Earth. Phosphate and Fe depletion, combined with Al immobility, has been used as an indicator of early terrestrial life in two very old basalt-derived paleosols, the Mount Roe (2.76 Ga) and the Hekpoort (2.25 Ga) paleosols [7]. P and Fe release and Y retention have been similarly interpreted in a 2.69 Ga tonalite paleosol [249]. Similarly, the mobilization of phosphate in the zone of intense formation of clay minerals (the top 30 cm of the paleosol) in a >503 Ma paleosol has been interpreted as a biosignature of mycorrhizal fungi [8]; similar mobilization of phosphate at the top of a weathering profile has also been observed in modern soils [250]. In contrast, the concentration of phosphorus in the top 150 cm of an Early Cambrian paleosol resembles the modern addition of phosphate [251]; this complex behavior has been described in terrestrial weathering profiles [252].

4.3.4. Microbially Mediated Biomineralization

Microbially mediated biomineralization occurs when microorganisms (bacteria, archaea, and algae) actively contribute to the formation of minerals. The morphology, texture, atomic structure, and chemical composition of minerals are influenced by their formation process, and as a result, minerals whose formation mechanism was impacted by life may contain information regarding their biological origin e.g., [11]. Therefore, minerals hold significant potential as valuable targets when searching for ancient signs of life in astrobiology [253,254]. Extracellular mineralization is defined as mineral formation that occurs outside or around a cell, and intracellular mineralization occurs when mineral formation occurs inside the cell. Biologically induced mineralization (BIM) is caused by passive microbial processes, and biologically controlled mineralization (BCM) is caused by active microbial processes.

4.3.5. Biologically Induced Mineralization (BIM)

Microbial cells contain significant phosphate, as much as 6% dry weight, e.g., [9], and many microorganisms have the ability to store phosphate in times of nutrient deprivation, e.g., [255]. This phosphate can serve as a valuable source of phosphorus for mineral formation in natural environments. For example, in laboratory experiments, Fe phosphate minerals can be formed on microbial surfaces [9–11], including with no source of phosphate other than the microbial cells themselves [9]. In addition, phosphate reserves in microbial cells have recently been postulated to contribute to the formation of apatite-rich phosphorite rocks on Earth [256–258].

Microorganisms in natural environments can become encrusted in phosphates, including iron phosphates, e.g., [259,260], potentially becoming entombed in such phosphates [261], which has been proposed as a mechanism for preservation in phosphorites on Earth [262]. Phosphate-rich molecules on microbial surfaces, such as teichoic acid, can bind to metals, as demonstrated by experiments that removed the phosphate-rich teichoic acid and resulted in less adsorption of metals onto the microbial surfaces [255]. Further experiments that tested the effects of diagenetic conditions on metal-adsorbed microbial cells showed the formation of phosphate-containing minerals, including Fe phosphates [9–11] (Figure 11). Phosphate-entombed evidence of microbial life has similarly been detected deep in the terrestrial rock record, e.g., [263,264], and Ca phosphates have also been shown to be formed in association with mineral surfaces and organic compounds [265], including the new mineral hazenite [266,267]. Phosphates are therefore important targets for sample collection on Mars [12,13].

4.3.6. Biologically Controlled Mineralization (BCM)

Because Ca- and phosphate-bearing minerals are important biominerals in higher organisms on Earth, multiple studies have examined the precipitation of Ca- and phosphate-containing minerals in the presence of organic compounds [268–283]. These studies have focused on larger, biotic molecules found in higher organisms rather than smaller, abiotic molecules, with previous studies showing molecules such as acid phospholipids, ameloginins, enamelin, and bone sialoprotein promoting the precipitation of hydroxyapatite; aggrecan, dentin matrix proteins, and osteopontin inhibiting hydroxyapatite precipitation; and many molecules, such as albumin, showing no effect [268–284]. Some studies have examined the effect of more environmentally relevant organic molecules such as phytic, mellitic, humic, and citric acids on the precipitation of dicalcium phosphate dihydrate [285]; fulvic, citric, tannic, and humic acids on octacalcium phosphate growth [286]; and the effect of acetate and citrate on hydroxyapatite precipitation [287]. All the molecules used in these three studies inhibited the precipitation of Ca and phosphate-containing compounds except acetate [285–287].

4.3.7. Oxygen Isotope Composition of Phosphate

Measurement of the mineralogy and chemistry of phosphate-containing phases in samples returned to Earth will provide unprecedented new information about the history of Mars. For example, previous work has shown the importance of the oxygen isotope composition of phosphate in elucidating different phosphate inputs and reaction pathways [18,288–300], P cycling processes [301–306], and its potential as a biosignature for Mars [301] in returned samples from Mars [307]. This critical tool will therefore be available for the analysis of phosphate upon sample return.
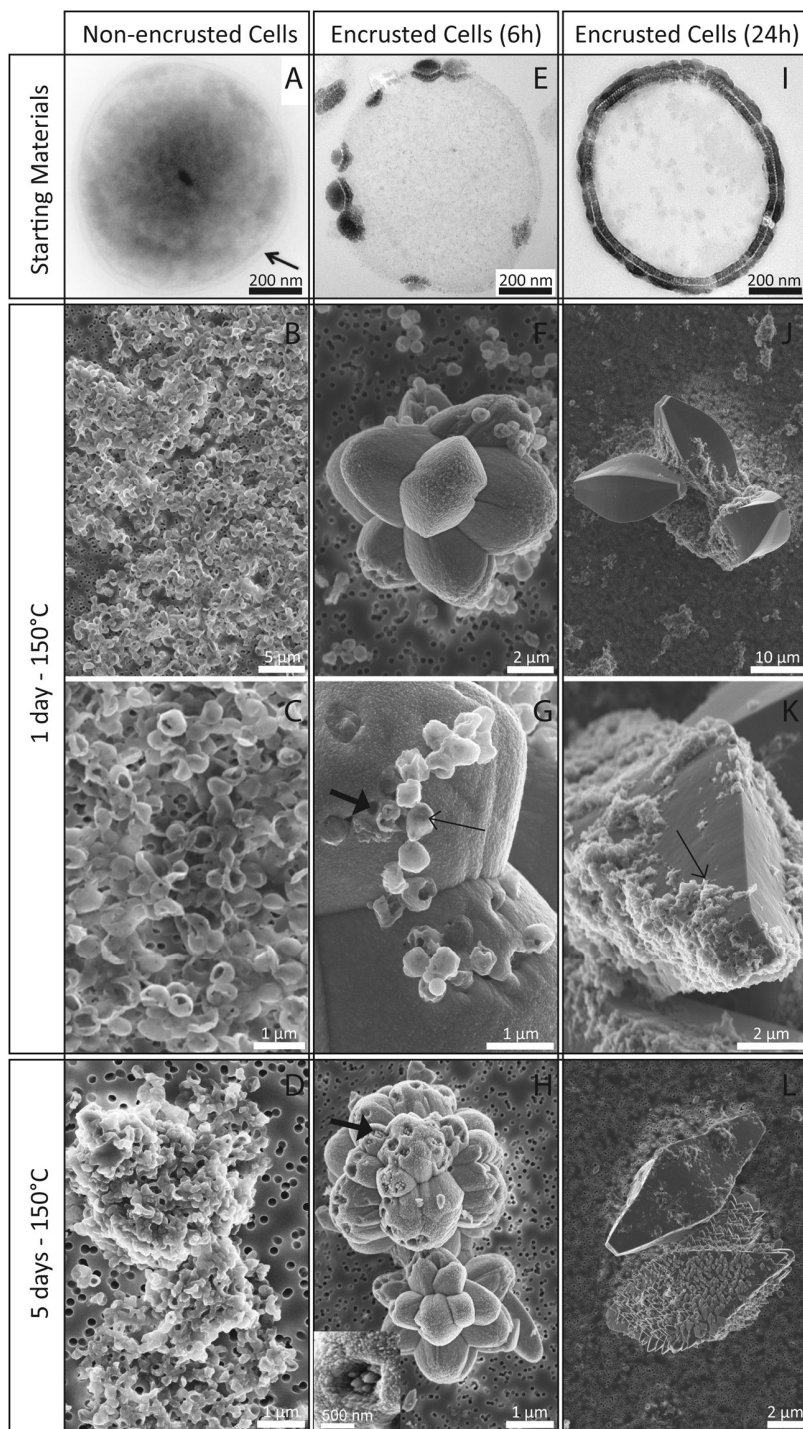
Figure 11. Images of non-encrusted and encrusted *S. acidocaldarius* cells A = non-encrusted cells starting materials, E = cells encrusted for 6 h starting materials, I = cells encrusted for 24 h starting materials, B and C = non-encrusted cells immersed in 2 mL of milliQ water at 150 °C for 1 day, D = non-encrusted cells immersed in 2 mL of milliQ water at 150 °C for 5 days, F, G = cells encrusted for 6 h immersed in 2 mL of milliQ water at 150 °C for 1 day, H = cells encrusted for 6 h immersed in 2 mL of milliQ water at 150 °C for 5 days, J, K = cells encrusted for 24 h immersed in 2 mL of milliQ water at 150 °C for 1 day, L = cells encrusted for 24 h cells immersed in 2 mL of milliQ water at 150 °C for 5 days. Thin arrows in G indicate non-mineralized vesicles and in K organic matter. Thick arrows in G and H point out pores in the surfaces of the framboids. Reproduced with permission from [11].

5. Conclusions and Future Work

In conclusion, phosphate minerals play a uniquely important role in the interpretation of Mars. They are crucial igneous indicators, preserving the volatile contents of magmas and their source regions. They are sensitive aqueous indicators, dissolving rapidly and forming different minerals under different conditions of temperature, pH, and composition. Finally, they are also very important as biological indicators. Phosphate is required by all known terrestrial life and has been used as biosignatures in ancient environments on Earth. The examination of phosphate on Mars and in samples returned from Mars is therefore critical in the interpretation of the igneous, aqueous, and potential biological past of that planet.

References

1. Madigan, M.T.; Martinko, J.M.; Parker, J. *Brock Biology of Microorganisms*; Prentice Hall: Upper Saddle River, NJ, USA, 2000.
2. Powner, M.W.; Gerland, B.; Sutherland, J.D. Synthesis of Activated Pyrimidine Ribonucleotides in Prebiotically Plausible Conditions. *Nature* **2009**, *459*, 239–242. [CrossRef]
3. Clark, F.E. *Terrestrial Nitrogen Cycles*; Clark, F.E., Rosswell, T., Eds.; Swedish Natural Science Research Council: Stockholm, Sweden, 1981; pp. 363–374.
4. Chadwick, O.A.; Derry, L.A.; Vitousek, P.M.; Huebert, B.J.; Hedin, L.O. Changing Sources of Nutrients during Four Million Years of Ecosystem Development. *Nature* **1999**, *397*, 491–497. [CrossRef]
5. Filippelli, G.M. The Global Phosphorus Cycle. *Rev. Mineral. Geochem.* **2002**, *48*, 391–425. [CrossRef]
6. Walker, T.W.; Syers, J.K. The Fate of Phosphorus during Pedogenesis. *Geoderma* **1976**, *15*, 1–19. [CrossRef]
7. Neaman, A.; Chorover, J.; Brantley, S.L. Element Mobility Patterns Record Organic Ligands in Soils on Early Earth. *Geology* **2005**, *33*, 117–120. [CrossRef]
8. Horodyskyj, L.B.; White, T.S.; Kump, L.R. Substantial Biologically Mediated Phosphorus Depletion from the Surface of a Middle Cambrian Paleosol. *Geology* **2012**, *40*, 503–506. [CrossRef]
9. Beveridge, T.J.; Meloche, J.D.; Fyfe, W.S.; Murray, R.G.E. Diagenesis of Metals Chemically Complexed to Bacteria: Laboratory Formation of Metal Phosphates, Sulfides, and Organic Condensates in Artificial Sediments. *Appl. Environ. Microbiol.* **1983**, *45*, 1094–1108. [CrossRef]
10. Kish, A.; Miot, J.; Lombard, C.; Guigner, J.-M.; Bernard, S.; Zirah, S.; Guyot, F. Preservation of Archaeal Surface Layer Structure During Mineralization. *Sci. Rep.* **2016**, *6*, 26152. [CrossRef]
11. Miot, J.; Bernard, S.; Bourreau, M.; Guyot, F.; Kish, A. Experimental Maturation of Archaea Encrusted by Fe-Phosphates. *Sci. Rep.* **2017**, *7*, 16984. [CrossRef]
12. Farmer, J.D.; Des Marais, D.J. Exploring for a Record of Ancient Martian Life. *J. Geophys. Res. Planets* **1999**, *104*, 26977–26995. [CrossRef]
13. Mojzsis, S.J.; Arrhenius, G. Phosphates and Carbon on Mars: Exobiological Implications and Sample Return Considerations. *J. Geophys. Res. Planets* **1998**, *103*, 28495–28511. [CrossRef]

14. McDonough, W.F.; Sun, S.-s. The Composition of the Earth. *Chem. Evol. Mantle* **1995**, *120*, 223–253. [CrossRef]
15. Taylor, G.J. The Bulk Composition of Mars. *Geochemistry* **2013**, *73*, 401–420. [CrossRef]
16. McCubbin, F.M.; Nekvasil, H. Maskelynite-Hosted Apatite in the Chassigny Meteorite. *Am. Mineral.* **2008**, *93*, 676–684. [CrossRef]
17. Bridges, J.C.; Grady, M.M. Evaporite Mineral Assemblages in the Nakhlite (Martian) Meteorites. *Earth Planet. Sci. Lett.* **2000**, *176*, 267–279. [CrossRef]
18. Greenwood, J.P.; Blake, R.E.; Coath, C.D. Ion Microprobe Measurements of $^{18}O/^{16}O$ Ratios of Phosphate Minerals in the Martian Meteorites ALH84001 and Los Angeles. *Geochim. Cosmochim. Acta* **2003**, *67*, 2289–2298. [CrossRef]
19. McSween, H.; Treiman, A.H. Martian Meteorites. In *Planetary Materials*; Papike, J., Ed.; Mineral Society of America: Washington, DC, USA, 1998; pp. F1–F53.
20. Barnes, J.J.; McCubbin, F.M.; Santos, A.R.; Day, J.M.D.; Boyce, J.W.; Schwenzer, S.P.; Ott, U.; Franchi, I.A.; Messenger, S.; Anand, M.; et al. Multiple Early-Formed Water Reservoirs in the Interior of Mars. *Nat. Geosci.* **2020**, *13*, 260–264. [CrossRef]
21. Brounce, M.; Boyce, J.W.; McCubbin, F.M. Sulfur in Apatite from the Nakhla Meteorite Record a Late-Stage Oxidation Event. *Earth Planet. Sci. Lett.* **2022**, *595*, 117784. [CrossRef]
22. Filiberto, J.; Gross, J.; McCubbin, F.M. Constraints on the Water, Chlorine, and Fluorine Content of the Martian Mantle. *Meteorit. Planet. Sci.* **2016**, *51*, 2023–2035. [CrossRef]
23. Filiberto, J.; Treiman, A.H. Martian Magmas Contained Abundant Chlorine, but Little Water. *Geology* **2009**, *37*, 1087–1090. [CrossRef]
24. Gross, J.; Filiberto, J.; Bell, A.S. Water in the Martian Interior: Evidence for Terrestrial MORB Mantle-like Volatile Contents from Hydroxyl-Rich Apatite in Olivine–Phyric Shergottite NWA 6234. *Earth Planet. Sci. Lett.* **2013**, *369–370*, 120–128. [CrossRef]
25. McCubbin, F.M.; Boyce, J.W.; Srinivasan, P.; Santos, A.R.; Elardo, S.M.; Filiberto, J.; Steele, A.; Shearer, C.K. Heterogeneous Distribution of H2O in the Martian Interior: Implications for the Abundance of H2O in Depleted and Enriched Mantle Sources. *Meteorit. Planet. Sci.* **2016**, *51*, 2036–2060. [CrossRef]
26. McCubbin, F.M.; Shearer, C.K.; Burger, P.V.; Hauri, E.H.; Wang, J.; Elardo, S.M.; Papike, J.J. Volatile Abundances of Coexisting Merrillite and Apatite in the Martian Meteorite Shergotty: Implications for Merrillite in Hydrous Magmas. *Am. Mineral.* **2014**, *99*, 1347–1354. [CrossRef]
27. McCubbin, F.M.; Elardo, S.M.; Shearer, C.K., Jr.; Smirnov, A.; Hauri, E.H.; Draper, D.S. A Petrogenetic Model for the Comagmatic Origin of Chassignites and Nakhlites: Inferences from Chlorine-Rich Minerals, Petrology, and Geochemistry. *Meteorit. Planet. Sci.* **2013**, *48*, 819–853. [CrossRef]
28. Shearer, C.K.; Messenger, S.; Sharp, Z.D.; Burger, P.V.; Nguyen, A.N.; McCubbin, F.M. Distinct Chlorine Isotopic Reservoirs on Mars. Implications for Character, Extent and Relative Timing of Crustal Interactions with Mantle-Derived Magmas, Evolution of the Martian Atmosphere, and the Building Blocks of an Early Mars. *Geochim. Cosmochim. Acta* **2018**, *234*, 24–36. [CrossRef]
29. Shearer, C.K.; Burger, P.V.; Papike, J.J.; McCubbin, F.M.; Bell, A.S. Crystal Chemistry of Merrillite from Martian Meteorites: Mineralogical Recorders of Magmatic Processes and Planetary Differentiation. *Meteorit. Planet. Sci.* **2015**, *50*, 649–673. [CrossRef]
30. Schmidt, M.E.; McCoy, T.J. The Evolution of a Heterogeneous Martian Mantle: Clues from K, P, Ti, Cr, and Ni Variations in Gusev Basalts and Shergottite Meteorites. *Earth Planet. Sci. Lett.* **2010**, *296*, 67–77. [CrossRef]
31. Adcock, C.T.; Hausrath, E.M.; Forster, P.M. Readily Available Phosphate from Minerals in Early Aqueous Environments on Mars. *Nat. Geosci.* **2013**, *6*, 824–827. [CrossRef]
32. Bridges, J.C.; Grady, M.M. A Halite-Siderite-Anhydrite-Chlorapatite Assemblage in Nakhla: Mineralogical Evidence for Evaporites on Mars. *Meteorit. Planet. Sci.* **1999**, *34*, 407–415. [CrossRef]
33. Greenwood, J.P.; Blake, R.E. Evidence for an Acidic Ocean on Mars from Phosphorus Geochemistry of Martian Soils and Rocks. *Geology* **2006**, *34*, 953–956. [CrossRef]
34. Kizovski, T.V.; Schmidt, M.E.; O'Neil, L.; Klevang, D.; Tosca, N.; Tice, M.; Cable, M.; Hausrath, E.; Adcock, C.T.; Hurowitz, J.; et al. *Fe-Phosphates in the Jezero Crater Fan: Implications for Habitability and Sample Return*; Lunar and Planetary Institute: Houston, TX, USA, 2024; p. Abstract #2615.
35. Lafuente, B.; Downs, R.T.; Yang, H.; Stone, N. *Highlights in Mineralogical Crystallography*; Armbruster, T., Danisi, R.M., Eds.; De Gruyter (O): Basel, Switzerland, 2016; pp. 1–30, ISBN 978-3-11-041710-4.
36. Economou, T. Chemical Analyses of Martian Soil and Rocks Obtained by the Pathfinder Alpha Proton X-ray Spectrometer. *Radiat. Phys. Chem.* **2001**, *61*, 191–197. [CrossRef]
37. Rieder, R.; Economou, T.; Wänke, H.; Turkevich, A.; Crisp, J.; Brückner, J.; Dreibus, G.; McSween, H.Y. The Chemical Composition of Martian Soil and Rocks Returned by the Mobile Alpha Proton X-ray Spectrometer: Preliminary Results from the X-ray Mode. *Science* **1997**, *278*, 1771–1774. [CrossRef]
38. Gellert, R.; Rieder, R.; Brückner, J.; Clark, B.C.; Dreibus, G.; Klingelhöfer, G.; Lugmair, G.; Ming, D.W.; Wänke, H.; Yen, A.; et al. Alpha Particle X-ray Spectrometer (APXS): Results from Gusev Crater and Calibration Report. *J. Geophys. Res. Planets* **2006**, *111*, E02S05. [CrossRef]
39. Usui, T.; McSween, H.Y., Jr.; Clark, B.C., III. Petrogenesis of High-Phosphorous Wishstone Class Rocks in Gusev Crater, Mars. *J. Geophys. Res. Planets* **2008**, *113*, E12S44. [CrossRef]
40. Rieder, R.; Gellert, R.; Anderson, R.C.; Bruckner, J.; Clark, B.C.; Dreibus, G.; Economou, T.; Klingelhofer, G.; Lugmair, G.W.; Ming, D.W.; et al. Chemistry of Rocks and Soils at Meridiani Planum from the Alpha Particle X-ray Spectrometer. *Science* **2004**, *306*, 1746–1749. [CrossRef]

41. Yen, A.S.; Ming, D.W.; Vaniman, D.T.; Gellert, R.; Blake, D.F.; Morris, R.V.; Morrison, S.M.; Bristow, T.F.; Chipera, S.J.; Edgett, K.S. Multiple Stages of Aqueous Alteration along Fractures in Mudstone and Sandstone Strata in Gale Crater, Mars. *Earth Planet. Sci. Lett.* **2017**, *471*, 186–198. [CrossRef]

42. Rampe, E.B.; Blake, D.F.; Bristow, T.F.; Ming, D.W.; Vaniman, D.T.; Morris, R.V.; Achilles, C.N.; Chipera, S.J.; Morrison, S.M.; Tu, V.M. Mineralogy and Geochemistry of Sedimentary Rocks and Eolian Sediments in Gale Crater, Mars: A Review after Six Earth Years of Exploration with Curiosity. *Geochemistry* **2020**, *80*, 125605. [CrossRef]

43. Nachon, M.; Mangold, N.; Forni, O.; Kah, L.C.; Cousin, A.; Wiens, R.C.; Anderson, R.; Blaney, D.; Blank, J.G.; Calef, F. Chemistry of Diagenetic Features Analyzed by ChemCam at Pahrump Hills, Gale Crater, Mars. *Icarus* **2017**, *281*, 121–136. [CrossRef]

44. Treiman, A.H.; Lanza, N.L.; VanBommel, S.; Berger, J.; Wiens, R.; Bristow, T.; Johnson, J.; Rice, M.; Hart, R.; McAdam, A. Manganese-Iron Phosphate Nodules at the Groken Site, Gale Crater, Mars. *Minerals* **2023**, *13*, 1122. [CrossRef]

45. VanBommel, S.J.; Berger, J.A.; Gellert, R.; O'Connell-Cooper, C.D.; McCraig, M.A.; Thompson, L.M.; Fedo, C.M.; Des Marais, D.J.; Fey, D.M.; Yen, A.S. Elemental Composition of Manganese-and Phosphorus-Rich Nodules in the Knockfarril Hill Member, Gale Crater, Mars. *Icarus* **2023**, *392*, 115372. [CrossRef]

46. Hausrath, E.M.; Sullivan, R.; Goreva, Y.; Zorzano, M.P.; Cardarelli, E.; Vaughan, A.; Cousin, A.; Siljestrom, S.; Shumway, A.; Van-Bommel, S.; et al. *The First Regolith Samples from Mars*; Lunar and Planetary Institute: Houston, TX, USA, 2023; p. Abstract #2379.

47. Herd, C.D.K.; Bosak, T.; Farley, K.A.; Stack, K.M.; Benison, K.C.; Cohen, B.A.; Czaja, A.D.; Debaille, V.; Goreva, Y.; Hausrath, E.M.; et al. *Sampling by the NASA Perseverance Rover for Mars Sample Return*; Lunar and Planetary Institute: Houston, TX, USA, 2023; p. Abstract #6140.

48. Simon, J.I.; Hickman-Lewis, K.; Cohen, B.A.; Mayhew, L.E.; Shuster, D.L.; Debaille, V.; Hausrath, E.M.; Weiss, B.P.; Bosak, T.; Zorzano, M.-P.; et al. Samples Collected From the Floor of Jezero Crater With the Mars 2020 Perseverance Rover. *J. Geophys. Res. Planets* **2023**, *128*, e2022JE007474. [CrossRef]

49. Gooding, J.L.; Wentworth, S.J.; Zolensky, M.E. Calcium Carbonate and Sulfate of Possible Extraterrestrial Origin in the EETA 79001 Meteorite. *Geochim. Cosmochim. Acta* **1988**, *52*, 909–915. [CrossRef]

50. Hurowitz, J.A.; McLennan, S.; Tosca, N.; Arvidson, R.; Michalski, J.R.; Ming, D.W.; Schroder, C.; Squyres, S.W. In Situ and Experimental Evidence for Acidic Weathering of Rocks and Soils on Mars. *J. Geophys. Res.* **2006**, *111*, E02S19. [CrossRef]

51. Ming, D.W.; Mittlefehldt, D.W.; Morris, R.V.; Golden, D.C.; Gellert, R.; Yen, A.; Clark, B.C.; Squyres, S.W.; Farrand, W.H.; Ruff, S.W.; et al. Geochemical and Mineralogical Indicators for Aqueous Processes in the Columbia Hills of Gusev Crater, Mars. *J. Geophys. Res.* **2006**, *111*, E02S12. [CrossRef]

52. Boanini, E.; Pagani, S.; Tschon, M.; Rubini, K.; Fini, M.; Bigi, A. Monetite vs. Brushite: Different Influences on Bone Cell Response Modulated by Strontium Functionalization. *J. Funct. Biomater.* **2022**, *13*, 65. [CrossRef]

53. Combes, C.; Cazalbou, S.; Rey, C. Apatite Biominerals. *Minerals* **2016**, *6*, 34. [CrossRef]

54. Dumitraş, D.-G.; Marincea, Ş.; Fransolet, A.-M. Brushite in the Bat Guano Deposit from the "Dry" Cioclovina Cave (Sureanu Mountains, Romania). *Neues Jahrb. Fuer Mineral. Abh.* **2004**, *180*, 45–64. [CrossRef]

55. Adcock, C.T.; Hausrath, E.M. Weathering Profiles in High-P Rocks at Gusev Crater, Mars, Suggest Dissolution of Phosphate Minerals into near-Neutral Waters. *Astrobiology* **2015**, *15*, 1060–1075. [CrossRef]

56. Rubin, A.; Ma, C. *Meteorite Mineralogy*; Cambridge University Press: Cambridge, UK, 2021; Volume 26.

57. Mathew, M.; Takagi, S. Structures of Biological Minerals in Dental Research. *J. Res. Natl. Inst. Stand. Technol.* **2001**, *106*, 1035. [CrossRef]

58. Lane, M.D.; Bishop, J.L.; Darby Dyar, M.; King, P.L.; Parente, M.; Hyde, B.C. Mineralogy of the Paso Robles Soils on Mars. *Am. Mineral.* **2008**, *93*, 728–739. [CrossRef]

59. Blake, D.F.; Morris, R.V.; Kocurek, G.; Morrison, S.M.; Downs, R.T.; Bish, D.; Ming, D.W.; Edgett, K.S.; Rubin, D.; Goetz, W.; et al. Curiosity at Gale Crater, Mars: Characterization and Analysis of the Rocknest Sand Shadow. *Science* **2013**, *341*, 1239505. [CrossRef]

60. Morris, R.V.; Vaniman, D.T.; Blake, D.F.; Gellert, R.; Chipera, S.J.; Rampe, E.B.; Ming, D.W.; Morrison, S.M.; Downs, R.T.; Treiman, A.H.; et al. Silicic Volcanism on Mars Evidenced by Tridymite in High-SiO2 Sedimentary Rock at Gale Crater. *Proc. Natl. Acad. Sci. USA* **2016**, *113*, 7071–7076. [CrossRef]

61. Achilles, C.N.; Downs, R.T.; Ming, D.W.; Rampe, E.B.; Morris, R.V.; Treiman, A.H.; Morrison, S.M.; Blake, D.F.; Vaniman, D.T.; Ewing, R.C.; et al. Mineralogy of an Active Eolian Sediment from the Namib Dune, Gale Crater, Mars. *J. Geophys. Res. Planets* **2017**, *122*, 2344–2361. [CrossRef]

62. Morrison, S.M.; Downs, R.T.; Blake, D.F.; Vaniman, D.T.; Ming, D.W.; Hazen, R.M.; Treiman, A.H.; Achilles, C.N.; Yen, A.S.; Morris, R.V.; et al. Crystal Chemistry of Martian Minerals from Bradbury Landing through Naukluft Plateau, Gale Crater, Mars. *Am. Mineral.* **2018**, *103*, 857–871. [CrossRef]

63. Morris, R.V.; Rampe, E.B.; Vaniman, D.T.; Christoffersen, R.; Yen, A.S.; Morrison, S.M.; Ming, D.W.; Achilles, C.N.; Fraeman, A.A.; Le, L.; et al. Hydrothermal Precipitation of Sanidine (Adularia) Having Full Al,Si Structural Disorder and Specular Hematite at Maunakea Volcano (Hawai'i) and at Gale Crater (Mars). *J. Geophys. Res. Planets* **2020**, *125*, e2019JE006324. [CrossRef]

64. McCubbin, F.M.; Jones, R.H. Extraterrestrial Apatite: Planetary Geochemistry to Astrobiology. *Elements* **2015**, *11*, 183–188. [CrossRef]

65. Pajor, K.; Pajchel, L.; Kolmas, J. Hydroxyapatite and Fluorapatite in Conservative Dentistry and Oral Implantology—A Review. *Materials* **2019**, *12*, 2683. [CrossRef]

66. Taylor, J.; Glover, E.; Ball, A.; Nojorka, J. Nanocrystalline Fluorapatite Mineralization in the Calciphile Rock-Boring Bivalve Lithophaga: Functional and Phylogenetic Significance. *Biol. J. Linn. Soc.* **2023**, *138*, 229–245. [CrossRef]

67. Adcock, C.T.; Hausrath, E.M.; Rampe, E.B.; Yang, H.; Downs, R.T. The Crystal Structure and Chemistry of Natural Giniite and Implications for Mars. *Am. Mineral.* **2023**, *108*, 430–438. [CrossRef]

68. Hausrath, E.M.; Tschauner, O. Natural Fumarolic Alteration of Fluorapatite, Olivine, and Basaltic Glass, and Implications for Habitable Environments on Mars. *Astrobiology* **2013**, *13*, 1049–1064. [CrossRef]

69. McCollom, T.M.; Donaldson, C.; Moskowitz, B.; Berquó, T.S.; Hynek, B. Phosphorous Immobility During Formation of the Layered Sulfate Deposits of the Burns Formation at Meridiani Planum. *J. Geophys. Res. Planets* **2018**, *123*, 1230–1254. [CrossRef]

70. Zheng, H.; Wang, X.; Lou, X.; Wang, Z.; Xing, B. Biochar-Induced Negative Carbon Mineralization Priming Effects in a Coastal Wetland Soil: Roles of Soil Aggregation and Microbial Modulation. *Sci. Total Environ.* **2018**, *610/611*, 951–960. [CrossRef]

71. Clark, B.C.; Van Hart, D.C. The Salts of Mars. *Icarus* **1981**, *45*, 370–378. [CrossRef]

72. LeGeros, R.Z.; LeGeros, J.P. Hydroxyapatite. In *Bioceramics and Their Clinical Applications*; Woodhead Publishing: Cambridge, UK, 2008; pp. 367–394, ISBN 978-1-84569-204-9.

73. Hench, L.L.; Thompson, I. Twenty-First Century Challenges for Biomaterials. *J. R. Soc. Interface* **2010**, *7*, S379–S391. [CrossRef]

74. Adcock, C.T.; Hausrath, E.M.; Forster, P.M.; Tschauner, O.; Sefein, K.J. Synthesis and Characterization of the Mars-Relevant Phosphate Minerals Fe-and Mg-Whitlockite and Merrillite and a Possible Mechanism That Maintains Charge Balance during Whitlockite to Merrillite Transformation. *Am. Mineral.* **2014**, *99*, 1221–1232. [CrossRef]

75. Thorpe, M.T.; Bristow, T.F.; Rampe, E.B.; Grotzinger, J.P.; Fox, V.K.; Bennett, K.A.; Bryk, A.B.; Yen, A.S.; Vasavada, A.R.; Vaniman, D.T. The Mineralogy and Sedimentary History of the Glen Torridon Region, Gale Crater, Mars. In Proceedings of the LPSC 2021, Houston, TX, USA, 15–19 March 2021.

76. Lanza, N.L.; Gasda, P.; Ari, E.; Comellas, J.; Caravaca, G.; Rampe, E.B.; Williams, A.J.; Meslin, P.-Y.; Dehouck, E.; Mangold, N. Chemistry of Manganese-Bearing Materials at the Groken Drill Site, Gale Crater, Mars. In Proceedings of the 52nd Lunar and Planetary Science Conference, Woodlands, TX, USA, 15–19 March 2021.

77. Drouet, C.; Loche, M.; Fabre, S.; Meslin, P.-Y. On the Occurrence of Jahnsite/Whiteite Phases on Mars: A Thermodynamic Study. *Am. Mineral.* **2022**, *107*, 1807–1817. [CrossRef]

78. Britvin, S.N.; Galuskina, I.O.; Vlasenko, N.S.; Vereshchagin, O.S.; Bocharov, V.N.; Krzhizhanovskaya, M.G.; Shilovskikh, V.V.; Galuskin, E.V.; Vapnik, Y.; Obolonskaya, E.V. Keplerite, Ca9(Ca0.5□0.5)Mg(PO4)7, a New Meteoritic and Terrestrial Phosphate Isomorphous with Merrillite, Ca9NaMg(PO4)7. *Am. Mineral.* **2021**, *106*, 1917–1927. [CrossRef]

79. Slabić, A. Shock-Induced Geochemical Variations in the Keplerite-Bearing Assemblages of Tissint and Intergrown Apatite-Merrillite Assemblages of ALH 84001, 146. PhD Thesis, University of Houston-Clear Lake, Houston, TX, USA, 2022.

80. Adcock, C.T.; Tschauner, O.; Hausrath, E.M.; Udry, A.; Luo, S.N.; Cai, Y.; Ren, M.; Lanzirotti, A.; Newville, M.; Kunz, M.; et al. Shock-Transformation of Whitlockite to Merrillite and the Implications for Meteoritic Phosphate. *Nat. Commun.* **2017**, *8*, 14667. [CrossRef]

81. Dorozhkin, S.V.; Epple, M. Biological and Medical Significance of Calcium Phosphates. *Angew. Chem. Int. Ed.* **2002**, *41*, 3130–3146. [CrossRef]

82. Weiner, S.; Wagner, H.D. THE MATERIAL BONE: Structure-Mechanical Function Relations. *Annu. Rev. Mater. Sci.* **1998**, *28*, 271–298. [CrossRef]

83. Gu, L.; Hu, S.; Anand, M.; Tang, X.; Ji, J.; Zhang, B.; Wang, N.; Lin, Y. Occurrence of Tuite and Ahrensite in Zagami and Their Significance for Shock-Histories Recorded in Martian Meteorites. *Am. Mineral.* **2022**, *107*, 1018–1029. [CrossRef]

84. Baziotis, I.P.; Liu, Y.; DeCarli, P.S.; Jay Melosh, H.; McSween, H.Y.; Bodnar, R.J.; Taylor, L.A. The Tissint Martian Meteorite as Evidence for the Largest Impact Excavation. *Nat. Commun.* **2013**, *4*, 1404. [CrossRef]

85. Tu, V.M.; Hausrath, E.M.; Tschauner, O.; Iota, V.; Egeland, G.W. Dissolution Rates of Amorphous Al- and Fe-Phosphates and Their Relevance to Phosphate Mobility on Mars†. *Am. Mineral.* **2014**, *99*, 1206–1215. [CrossRef]

86. Ruff, S.W.; Hamilton, V.E. Wishstone to Watchtower: Amorphous Alteration of Plagioclase-Rich Rocks in Gusev Crater, Mars. *Am. Mineral.* **2017**, *102*, 235–251. [CrossRef]

87. Ehrlich, H.L. Microbes as Geologic Agents: Their Role in Mineral Formation. *Geomicrobiol. J.* **1999**, *16*, 135–153. [CrossRef]

88. Hazen, R.M.; Downs, R.T.; Morrison, S.M.; Tutolo, B.M.; Blake, D.F.; Bristow, T.F.; Chipera, S.J.; McSween, H.Y.; Ming, D.; Morris, R.V.; et al. On the Diversity and Formation Modes of Martian Minerals. *J. Geophys. Res. Planets* **2023**, *128*, e2023JE007865. [CrossRef]

89. Brady, M.P.; Tostevin, R.; Tosca, N.J. Marine Phosphate Availability and the Chemical Origins of Life on Earth. *Nat. Commun.* **2022**, *13*, 5162. [CrossRef]

90. Rothe, M.; Kleeberg, A.; Hupfer, M. The Occurrence, Identification and Environmental Relevance of Vivianite in Waterlogged Soils and Aquatic Sediments. *Earth-Sci. Rev.* **2016**, *158*, 516–564. [CrossRef]

91. Jang, H.L.; Jin, K.; Lee, J.; Kim, Y.; Nahm, S.H.; Hong, K.S.; Nam, K.T. Revisiting Whitlockite, the Second Most Abundant Biomineral in Bone: Nanocrystal Synthesis in Physiologically Relevant Conditions and Biocompatibility Evaluation. *ACS Nano* **2014**, *8*, 634–641. [CrossRef]

92. Liu, Y.; Ma, C.; Beckett, J.R.; Chen, Y.; Guan, Y. Rare-Earth-Element Minerals in Martian Breccia Meteorites NWA 7034 and 7533: Implications for Fluid–Rock Interaction in the Martian Crust. *Earth Planet. Sci. Lett.* **2016**, *451*, 251–262. [CrossRef]

93. do Nascimento-Dias, B.L. Combination between Ca, P and Y in the Martian Meteorite NWA 6963 Could Be Used as a Strategy to Indicate Liquid Water Reservoirs on Ancient Mars? *Int. J. Astrobiol.* **2019**, *18*, 151–156. [CrossRef]

94. McSween, H.Y., Jr. SNC Meteorites: Are They Martian Rocks? *Geology* **1984**, *12*, 3–6. [CrossRef]

95. McSween, H.Y. What We Have Learned about Mars from SNC Meteorites. *Meteoritics* **1994**, *29*, 757–779. [CrossRef]

96. Warren, P.H. Lunar and Martian Meteorite Delivery Services. *Icarus* **1994**, *111*, 338–363. [CrossRef]

97. Gattacceca, J.; McCubbin, F.M.; Grossman, J.N.; Schrader, D.L.; Chabot, N.L.; D'Orazio, M.; Goodrich, C.; Greshake, A.; Gross, J.; Joy, K.H.; et al. The Meteoritical Bulletin, No. 111. *Meteorit. Planet. Sci.* **2023**, *58*, 901–904. [CrossRef]

98. Bogard, D.D.; Johnson, P. Martian Gases in an Antartic Meteorite? *Science* **1983**, *221*, 651–654. [CrossRef]

99. McSween, H.Y. Petrology on Mars. *Am. Mineral.* **2015**, *100*, 2380–2395. [CrossRef]

100. Udry, A.; Howarth, G.H.; Herd, C.D.K.; Day, J.M.D.; Lapen, T.J.; Filiberto, J. What Martian Meteorites Reveal About the Interior and Surface of Mars. *J. Geophys. Res. Planets* **2020**, *125*, 1–34. [CrossRef]

101. Agee, C.B.; Wilson, N.V.; McCubbin, F.M.; Ziegler, K.; Polyak, V.J.; Sharp, Z.D.; Asmerom, Y.; Nunn, M.H.; Shaheen, R.; Thiemens, M.H.; et al. Unique Meteorite from Early Amazonian Mars: Water-Rich Basaltic Breccia Northwest Africa 7034. *Science* **2013**, *339*, 780–785. [CrossRef]

102. Humayun, M.; Nemchin, A.; Zanda, B.; Hewins, R.H.; Grange, M.; Kennedy, A.; Lorand, J.P.; Göpel, C.; Fieni, C.; Pont, S.; et al. Origin and Age of the Earliest Martian Crust from Meteorite NWA 7533. *Nature* **2013**, *503*, 513–516. [CrossRef]

103. Britvin, S.N.; Krivovichev, S.V.; Armbruster, T. Ferromerrillite, Ca9NaFe2+(PO4)7, a New Mineral from the Martian Meteorites, and Some Insights into Merrillite–Tuite Transformation in Shergottites. *Eur. J. Mineral.* **2016**, *28*, 125–136. [CrossRef]

104. Hughes, J.M.; Jolliff, B.L.; Rakovan, J. The Crystal Chemistry of Whitlockite and Merrillite and the Dehydrogenation of Whitlockite to Merrillite. *Am. Mineral.* **2008**, *93*, 1300–1305. [CrossRef]

105. Hughes, J.M.; Jolliff, B.L.; Gunter, M.E. The Atomic Arrangement of Merrillite from the Fra Mauro Formation, Apollo 14 Lunar Mission: The First Structure of Merrillite from the Moon. *Am. Mineral.* **2006**, *91*, 1547–1552. [CrossRef]

106. Jolliff, B.L.; Hughes, J.M.; Freeman, J.J.; Zeigler, R.A. Crystal Chemistry of Lunar Merrillite and Comparison to Other Meteoritic and Planetary Suites of Whitlockite and Merrillite. *Am. Mineral.* **2006**, *91*, 1583–1595. [CrossRef]

107. Dowty, E. Phosphate in Angra Dos Reis: Structure and Composition of the Ca3 (PO4)2 Minerals. *Earth Planet. Sci. Lett.* **1977**, *35*, 347–351. [CrossRef]

108. Ionov, D.; Hofmann, A.; Merlet, C.; Gurenko, A.; Hellebrand, E.; Montagnac, G.; Gillet, P.; Prikhodko, V. Discovery of Whitlockite in Mantle Xenoliths: Inferences for Water- and Halogen-Poor Fluids and Trace Element Residence in the Terrestrial Upper Mantle. *Earth Planet. Sci. Lett.* **2006**, *244*, 201–217. [CrossRef]

109. Kaminsky, F.V.; Zedgenizov, D.A. First Find of Merrillite, Ca3(PO4)2, in a Terrestrial Environment as an Inclusion in Lower-Mantle Diamond. *Am. Mineral.* **2022**, *107*, 1652–1655. [CrossRef]

110. McCubbin, F.M.; Phillips, B.L.; Adcock, C.T.; Tait, K.T.; Steele, A.; Vaughn, J.S.; Fries, M.D.; Atudorei, V.; Vander Kaaden, K.E.; Hausrath, E.M. Discreditation of Bobdownsite and the Establishment of Criteria for the Identification of Minerals with Essential Monofluorophosphate (PO3F2–). *Am. Mineral.* **2018**, *103*, 1319–1328. [CrossRef]

111. Frondel, C. Whitlockite: A New Calcium Phosphate, Ca3(PO4)2. *Am. Mineral.* **1941**, *26*, 145–152.

112. Howarth, G.H.; Liu, Y.; Chen, Y.; Pernet-Fisher, J.F.; Taylor, L.A. Postcrystallization Metasomatism in Shergottites: Evidence from the Paired Meteorites LAR 06319 and LAR 12011. *Meteorit. Planet. Sci.* **2016**, *51*, 2061–2072. [CrossRef]

113. McCubbin, F.M.; Boyce, J.W.; Novák-Szabó, T.; Santos, A.R.; Tartèse, R.; Muttik, N.; Domokos, G.; Vazquez, J.; Keller, L.P.; Moser, D.E.; et al. Geologic History of Martian Regolith Breccia Northwest Africa 7034: Evidence for Hydrothermal Activity and Lithologic Diversity in the Martian Crust: Geologic History of NWA 7034. *J. Geophys. Res. Planets* **2016**, *121*, 2120–2149. [CrossRef]

114. Santos, A.R.; Agee, C.B.; McCubbin, F.M.; Shearer, C.K.; Burger, P.V.; Tartèse, R.; Anand, M. Petrology of Igneous Clasts in Northwest Africa 7034: Implications for the Petrologic Diversity of the Martian Crust. *Geochim. Cosmochim. Acta* **2015**, *157*, 56–85. [CrossRef]

115. Hu, S.; Lin, Y.; Zhang, J.; Hao, J.; Xing, W.; Zhang, T.; Yang, W.; Changela, H. Ancient Geologic Events on Mars Revealed by Zircons and Apatites from the Martian Regolith Breccia NWA 7034. *Meteorit. Planet. Sci.* **2019**, *54*, 850–879. [CrossRef]

116. Xie, X.; Zhai, S.; Chen, M.; Yang, H. Tuite, γ-Ca3(PO4)2, Formed by Chlorapatite Decomposition in a Shock Vein of the Suizhou L6 Chondrite. *Meteorit. Planet. Sci.* **2013**, *48*, 1515–1523. [CrossRef]

117. Xie, X.; Minitti, M.E.; Chen, M.; Mao, H.-K.; Wang, D.; Shu, J.; Fei, Y. Tuite, γ-Ca3(PO4)2: A New Mineral from the Suizhou L6 Chondrite. *Eur. J. Mineral.* **2003**, *15*, 1001–1005. [CrossRef]

118. Balta, J.B.; Sanborn, M.E.; McSween, H.Y.; Wadhwa, M. Magmatic History and Parental Melt Composition of Olivine-Phyric Shergottite LAR 06319. *Meteorit Planet Sci* **2013**, *48*, 1359–1382. [CrossRef]

119. Chowdhury, P.; Brounce, M.; Boyce, J.W.; McCubbin, F.M. The Oxidation State of Sulfur in Apatite of Martian Meteorite—Shergotty. *J. Geophys. Res. Planets* **2023**, *128*, e2022JE007634. [CrossRef]

120. Darling, J.R.; White, L.F.; Kizovski, T.; Černok, A.; Moser, D.E.; Tait, K.T.; Dunlop, J.; Langelier, B.; Douglas, J.O.; Zhao, X.; et al. The Shocking State of Apatite and Merrillite in Shergottite Northwest Africa 5298 and Extreme Nanoscale Chlorine Isotope Variability Revealed by Atom Probe Tomography. *Geochim. Cosmochim. Acta* **2021**, *293*, 422–437. [CrossRef]

121. Gross, J.; Filiberto, J.; Herd, C.D.; Daswani, M.M.; Schwenzer, S.P.; Treiman, A.H. Petrography, Mineral Chemistry, and Crystallization History of Olivine-phyric Shergottite NWA 6234: A New Melt Composition. *Meteorit. Planet. Sci.* **2013**, *48*, 854–871. [CrossRef]

122. Hu, S.; Lin, Y.; Anand, M.; Franchi, I.A.; Zhao, X.; Zhang, J.; Hao, J.; Zhang, T.; Yang, W.; Changela, H. Deuterium and 37Chlorine Rich Fluids on the Surface of Mars: Evidence From the Enriched Basaltic Shergottite Northwest Africa 8657. *J. Geophys. Res. Planets* **2020**, *125*, 1–15. [CrossRef]

123. Hu, S.; Lin, Y.; Zhang, J.; Hao, J.; Feng, L.; Xu, L.; Yang, W.; Yang, J. NanoSIMS Analyses of Apatite and Melt Inclusions in the GRV 020090 Martian Meteorite: Hydrogen Isotope Evidence for Recent Past Underground Hydrothermal Activity on Mars. *Geochim. Cosmochim. Acta* **2014**, *140*, 321–333. [CrossRef]

124. McCubbin, F.M.; Hauri, E.H.; Elardo, S.M.; Vander Kaaden, K.E.; Wang, J.; Shearer, C.K., Jr. Hydrous Melting of the Martian Mantle Produced Both Depleted and Enriched Shergottites. *Geology* **2012**, *40*, 683–686. [CrossRef]

125. Slaby, E.; Koch-Mueller, M.; Foerster, H.-J.; Wirth, R.; Rhede, D.; Schreiber, A.; Schade, U. Determination of Volatile Concentrations in Fluorapatite of Martian Shergottite NWA 2975 by Combining Synchrotron FTIR, Raman Spectroscopy, EMPA, and TEM, and Inferences on the Volatile Budget of the Apatite Host-Magma. *Meteorit Planet Sci* **2016**, *51*, 390–406. [CrossRef]

126. Hewins, R.H.; Humayun, M.; Barrat, J.A.; Zanda, B.; Lorand, J.P.; Pont, S.; Assayag, N.; Cartigny, P.; Yang, S.; Sautter, V. Northwest Africa 8694, a Ferroan Chassignite. *Geochim. Cosmochim. Acta* **2020**, *282*, 201–226. [CrossRef]

127. Birski, L.; Slaby, E.; Chatzitheodoridis, E.; Wirth, R.; Majzner, K.; Kozub-Budzyn, G.A.; Slama, J.; Liszewska, K.M.; Kocjan, I.; Zagorska, A. Apatite from NWA 10153 and NWA 10645-the Key to Deciphering Magmatic and Fluid Evolution History in Nakhlites. *Minerals* **2019**, *9*, 695. [CrossRef]

128. Davidson, J.; Wadhwa, M.; Hervig, R.L.; Stephant, A. Water on Mars. *Earth Planet Sci. Lett.* **2020**, *552*, 116597. [CrossRef]

129. Boctor, N.Z.; Alexander, C.M.O.; Wang, J.; Hauri, E. The Sources of Water in Martian Meteorites. *Geochim. Cosmochim. Acta* **2003**, *67*, 3971–3989. [CrossRef]

130. Baird, A.K.; Toulmin, P., 3rd; Clark, B.C.; Rose, H.J.J.; Keil, K.; Christian, R.P.; Gooding, J.L. Mineralogic and Petrologic Implications of Viking Geochemical Results from Mars: Interim Report. *Science* **1976**, *194*, 1288–1293. [CrossRef]

131. Clark, B.C. Geochemical Components in Martian Soil. *Geochim. Cosmochim. Acta* **1993**, *57*, 4575–4581. [CrossRef]

132. Clark, B.C.; Baird, A.K.; Weldon, R.J.; Tsusaki, D.M.; Schnabel, L.; Candelaria, M.P. Chemical Composition of Martian Fines. *J. Geophys. Res. Solid Earth* **1982**, *87*, 10059–10067. [CrossRef]

133. Clark, B.C.; Baird, A.K.; Rose, H.J.; Toulmin, P.; Keil, K.; Castro, A.J.; Kelliher, W.C.; Rowe, C.D.; Evans, P.H. Inorganic Analyses of Martian Surface Samples at the Viking Landing Sites. *Science* **1976**, *194*, 1283–1288. [CrossRef]

134. Brückner, J.; Dreibus, G.; Rieder, R.; Wänke, H. Refined Data of Alpha Proton X-ray Spectrometer Analyses of Soils and Rocks at the Mars Pathfinder Site: Implications for Surface Chemistry. *J. Geophys. Res.* **2003**, *108*, 8094. [CrossRef]

135. Foley, C.N.; Economou, T.; Clayton, R.N. Final Chemical Results from the Mars Pathfinder Alpha Proton X-ray Spectrometer. *J. Geophys. Res. Planets* **2003**, *108*, 8096. [CrossRef]

136. Kounaves, S.P.; Hecht, M.H.; West, S.J.; Morookian, J.M.; Young, S.M.M.; Quinn, R.; Grunthaner, P.; Wen, X.; Weilert, M.; Cable, C.A. The MECA Wet Chemistry Laboratory on the 2007 Phoenix Mars Scout Lander. *J. Geophys. Res.* **2009**, *114*, E00A19. [CrossRef]

137. Hurowitz, J.A.; McLennan, S.M.; McSween, H.Y.; DeSouza, P.A.J.; Klingelhofer, G. Mixing Relationships and the Effects of Secondary Alteration in the Wishstone and Watchtower Classes of Husband Hill, Gusev Crater, Mars. *J. Geophys. Res.* **2006**, *111*, E12S14. [CrossRef]

138. Gellert, R.; Rieder, R.; Anderson, R.C.; Bruckner, J.; Clark, B.C.; Dreibus, G.; Economou, T.; Klingelhofer, G.; Lugmair, G.W.; Ming, D.W.; et al. Chemistry of Rocks and Soils in Gusev Crater from the Alpha Particle X-ray Spectrometer. *Science* **2004**, *305*, 829–832. [CrossRef]

139. Ruff, S.W.; Christensen, P.R.; Blaney, D.L.; Farrand, W.H.; Johnson, J.R.; Michalski, J.R.; Moersch, J.E.; Wright, S.P.; Squyres, S.W. The Rocks of Gusev Crater as Viewed by the Mini-TES Instrument. *J. Geophys. Res.* **2006**, *111*, E12S18. [CrossRef]

140. Hausrath, E.M.; Golden, D.C.; Morris, R.V.; Agresti, D.G.; Ming, D.W. Acid Sulfate Alteration of Fluorapatite, Basaltic Glass and Olivine by Hydrothermal Vapors and Fluids: Implications for Fumarolic Activity and Secondary Phosphate Phases in Sulfate-Rich Paso Robles Soil at Gusev Crater, Mars. *J. Geophys. Res. Planets* **2013**, *118*, 1–13. [CrossRef]

141. Gellert, R.; Yen, A.S. Elemental Analyses of Mars from Rovers Using the Alpha-Particle X-ray Spectrometer. In *Remote Compositional Analysis: Techniques for Understanding Spectroscopy, Mineralogy, and Geochemistry of Planetary Surfaces*; Cambridge University Press: Cambridge, UK, 2019; pp. 555–572, ISBN 978-1-107-18620-0.

142. Arvidson, R.E.; Squyres, S.W.; Morris, R.V.; Knoll, A.H.; Gellert, R.; Clark, B.C.; Catalano, J.G.; Jolliff, B.L.; McLennan, S.M.; Herkenhoff, K.E.; et al. High Concentrations of Manganese and Sulfur in Deposits on Murray Ridge, Endeavour Crater, Mars. *Am. Mineral.* **2016**, *101*, 1389–1405. [CrossRef]

143. Rampe, E.B.; Bristow, T.F.; Morris, R.V.; Morrison, S.M.; Achilles, C.N.; Ming, D.W.; Vaniman, D.T.; Blake, D.F.; Tu, V.M.; Chipera, S.J.; et al. Mineralogy of Vera Rubin Ridge From the Mars Science Laboratory CheMin Instrument. *J. Geophys. Res. Planets* **2020**, *125*, e2019JE006306. [CrossRef]

144. Forni, O.; Gaft, M.; Toplis, M.J.; Clegg, S.M.; Maurice, S.; Wiens, R.C.; Mangold, N.; Gasnault, O.; Sautter, V.; Le Mouélic, S.; et al. First Detection of Fluorine on Mars: Implications for Gale Crater's Geochemistry. *Geophys. Res. Lett.* **2015**, *42*, 1020–1028. [CrossRef]

145. Hausrath, E.M.; Ming, D.W.; Rampe, E.B.; Peretyazhko, T.S. Reactive Transport Modeling of Aqueous Alteration in the Murray Formation, Gale Crater, Mars. *ACS Earth Space Chem.* **2021**, *5*, 424–435. [CrossRef]

146. Rampe, E.B.; Ming, D.W.; Blake, D.F.; Bristow, T.F.; Chipera, S.J.; Grotzinger, J.P.; Morris, R.V.; Morrison, S.M.; Vaniman, D.T.; Yen, A.S.; et al. Mineralogy of an Ancient Lacustrine Mudstone Succession from the Murray Formation, Gale Crater, Mars. *Earth Planet. Sci. Lett.* **2017**, *471*, 172–185. [CrossRef]

147. Dehouck, E.; McLennan, S.M.; Meslin, P.-Y.; Cousin, A. Constraints on Abundance, Composition, and Nature of X-ray Amorphous Components of Soils and Rocks at Gale Crater, Mars. *J. Geophys. Res. Planets* **2014**, *119*, 2640–2657. [CrossRef]

148. Smith, R.J.; McLennan, S.M.; Achilles, C.N.; Dehouck, E.; Horgan, B.H.N.; Mangold, N.; Rampe, E.B.; Salvatore, M.; Siebach, K.L.; Sun, V. X-ray Amorphous Components in Sedimentary Rocks of Gale Crater, Mars: Evidence for Ancient Formation and Long-Lived Aqueous Activity. *J. Geophys. Res. Planets* **2021**, *126*, e2020JE006782. [CrossRef]

149. Achilles, C.N.; Sutter, B.; Lybrand, R.; Ming, D.W.; McAdam, A.C.; Zaharescu, G.D.; Morse, Z.; Honniball, C.; Whelley, P.; Richardson, J.; et al. *Investigating Icelandic Soils as an Analog for Pedogenic Processes on Mars*; Lunar and Planetary Institute: Houston, TX, USA, 2022; p. Abstract #2472.

150. Pandey, A.; Rampe, E.; Morris, R.V.; Peretyazhko, T.; Niles, P.B.; Archer, D.A.; Casbeer, P.; Clark, J.; Sutter, B.; Chipera, S.J.; et al. *Cryo-Formation of Sulfate Salts: Implications for Ancient Aqueous Environments on Mars*; Lunar and Planetary Institute: Houston, TX, USA, 2024; p. Abstract #2301.

151. Berger, J.A.; Gellert, R.; Boyd, N.I.; King, P.L.; McCraig, M.A.; O'Connell-Cooper, C.D.; Schmidt, M.E.; Spray, J.G.; Thompson, L.M.; VanBommel, S.J.V.; et al. Elemental Composition and Chemical Evolution of Geologic Materials in Gale Crater, Mars: APXS Results from Bradbury Landing to the Vera Rubin Ridge. *J. Geophys. Res. Planets* **2020**, *125*, e2020JE006536. [CrossRef]

152. Achilles, C.N.; Rampe, E.B.; Downs, R.T.; Bristow, T.F.; Ming, D.W.; Morris, R.V.; Vaniman, D.T.; Blake, D.F.; Yen, A.S.; McAdam, A.C.; et al. Evidence for Multiple Diagenetic Episodes in Ancient Fluvial-Lacustrine Sedimentary Rocks in Gale Crater, Mars. *J. Geophys. Res. Planets* **2020**, *125*, e2019JE006295. [CrossRef]

153. Meslin, P.-Y.; Gasda, P.; L'Haridon, J.; Forni, O.; Lanza, N.; Lamm, S.; Johnson, J.R.; Wiens, R.C.; Thompson, L.; Rapin, W.; et al. Detection of Hydrous Manganese and Iron Oxides with Variable Phosphorus and Magnesium Contents in the Lacustrine Sediments of the Murray Formation, Gale, Mars. In Proceedings of the 49th Lunar and Planetary Science Conference, Houston, TX, USA, 19–23 March 2018.

154. Berger, J.A. Supporting Information Document for Manganese Mobility in Gale Crater, Mars: Leached Bedrock and Localized Enrichments. *J. Geophys. Res. Planets* **2022**, *127*, e2021JE007171. [CrossRef]

155. Berger, J.A.; Schmidt, M.E.; Izawa, M.R.M.; Gellert, R.; Ming, D.W.; Rampe, E.B.; VanBommel, S.J.; McAdam, A.C. Phosphate Stability in Diagenetic Fluids Constrains the Acidic Alteration Model for Lower Mt. Sharp Sedimentary Rocks in Gale Crater, Mars. In Proceedings of the 47th Lunar and Planetary Science Conference, Woodlands, TX, USA, 21–25 March 2016.

156. Berger, J.A.; Ming, D.W.; Morris, R.V.; Peretyazhko, T.; Rampe, E.B.; Schmidt, M.E.; Tu, V. Importance of Sulfur for Phosphorus Mobility on the Martian Surface. In Proceedings of the AGU Fall Meeting 2022, Chicago, IL, USA, 12–16 December 2022; Volume 2022, p. P12C-01.

157. Berger, J.A.; Ming, D.W.; Morris, R.V.; King, P.L.; Schmidt, M.E.; Tu, V.M. Aluminum Phosphate-Sulfate Minerals: The Fate of Mobile Phosphorus in Sulfur-Rich, Mars-Relevant Systems. In Proceedings of the 51st Lunar and Planetary Science Conference, Woodlands, TX, USA, 16–20 March 2020.

158. Kronyak, R.E.; Kah, L.C.; Edgett, K.S.; Van Bommel, S.J.; Thompson, L.M.; Wiens, R.C.; Sun, V.Z.; Nachon, M. Mineral-Filled Fractures as Indicators of Multigenerational Fluid Flow in the Pahrump Hills Member of the Murray Formation, Gale Crater, Mars. *Earth Space Sci.* **2019**, *6*, 238–265. [CrossRef]

159. Yen, A.S.; Morris, R.V.; Ming, D.W.; Schwenzer, S.P.; Sutter, B.; Vaniman, D.T.; Treiman, A.H.; Gellert, R.; Achilles, C.N.; Berger, J.A.; et al. Formation of Tridymite and Evidence for a Hydrothermal History at Gale Crater, Mars. *J. Geophys. Res. Planets* **2021**, *126*, e2020JE006569. [CrossRef]

160. Hausrath, E.M.; Ming, D.W.; Peretyazhko, T.S.; Rampe, E.B. Reactive Transport and Mass Balance Modeling of the Stimson Sedimentary Formation and Altered Fracture Zones Constrain Diagenetic Conditions at Gale Crater, Mars. *Earth Planet. Sci. Lett.* **2018**, *491*, 1–10. [CrossRef]

161. Farley, K.A.; Williford, K.H.; Stack, K.M.; Bhartia, R.; Chen, A.; de la Torre, M.; Hand, K.; Goreva, Y.; Herd, C.D.K.; Hueso, R.; et al. Mars 2020 Mission Overview. *Space Sci. Rev.* **2020**, *216*, 142. [CrossRef]

162. Udry, A.; Ostwald, A.; Sautter, V.; Cousin, A.; Beyssac, O.; Forni, O.; Dromart, G.; Benzerara, K.; Nachon, M.; Horgan, B.; et al. A Mars 2020 Perseverance SuperCam Perspective on the Igneous Nature of the Máaz Formation at Jezero Crater and Link With Séítah, Mars. *J. Geophys. Res. Planets* **2023**, *128*, e2022JE007440. [CrossRef]

163. Beyssac, O.; Forni, O.; Cousin, A.; Udry, A.; Kah, L.C.; Mandon, L.; Clavé, O.E.; Liu, Y.; Poulet, F.; Quantin Nataf, C.; et al. Petrological Traverse of the Olivine Cumulate Séítah Formation at Jezero Crater, Mars: A Perspective From SuperCam Onboard Perseverance. *J. Geophys. Res. Planets* **2023**, *128*, e2022JE007638. [CrossRef]

164. Scheller, E.L.; Razzell Hollis, J.; Cardarelli, E.L.; Steele, A.; Beegle, L.W.; Bhartia, R.; Conrad, P.; Uckert, K.; Sharma, S.; Ehlmann, B.L.; et al. Aqueous Alteration Processes in Jezero Crater, Mars—Implications for Organic Geochemistry. *Science* **2022**, *378*, 1105–1110. [CrossRef]

165. Kizovski, T.V.; Schmidt, M.E.; Liu, Y.; Clark, B.C.; Tice, M.; Herd, C.D.K.; Hurowitz, J.; VanBommel, S.; Henley, T.; Allwood, A. *Minor Minerals Analyzed by PIXL—A Major Part of Igneous Rock Petrogenesis at Jezero Crater*; Lunar and Planetary Institute: Houston, TX, USA, 2022; p. Abstract #2384.

166. Kizovski, T.V.; O'Neil, L.; Schmidt, M.; Hurowitz, J.; Treiman, A.; Pedersen, D.; Liu, Y.; Tice, M.; Herd, C.; Labrie, J.; et al. *Minor Minerals in the Jezero Crater Delta Analyzed by PIXL—Provenance and Mars Sample Return Implications*; Lunar and Planetary Institute: Houston, TX, USA, 2023; p. Abstract #2855.

167. Liu, Y.; Tice, M.M.; Schmidt, M.E.; Treiman, A.H.; Kizovski, T.V.; Hurowitz, J.A.; Allwood, A.C.; Henneke, J.; Pedersen, D.A.K.; VanBommel, S.J.; et al. An Olivine Cumulate Outcrop on the Floor of Jezero Crater, Mars. *Science* **2022**, *377*, 1513–1519. [CrossRef]

168. Allwood, A.C.; Wade, L.A.; Foote, M.C.; Elam, W.T.; Hurowitz, J.A.; Battel, S.; Dawson, D.E.; Denise, R.W.; Ek, E.M.; Gilbert, M.S.; et al. PIXL: Planetary Instrument for X-ray Lithochemistry. *Space Sci. Rev.* **2020**, *216*, 134. [CrossRef]

169. Farley, K.A.; Stack, K.M.; Shuster, D.L.; Horgan, B.H.N.; Hurowitz, J.A.; Tarnas, J.D.; Simon, J.I.; Sun, V.Z.; Scheller, E.L.; Moore, K.R.; et al. Aqueously Altered Igneous Rocks Sampled on the Floor of Jezero Crater, Mars. *Science* **2022**, *377*, eabo2196. [CrossRef]

170. Tice, M.M.; Hurowitz, J.A.; Allwood, A.C.; Jones, M.W.M.; Orenstein, B.J.; Davidoff, S.; Wright, A.P.; Pedersen, D.A.K.; Henneke, J.; Tosca, N.J.; et al. Alteration History of Séítah Formation Rocks Inferred by PIXL X-ray Fluorescence, X-ray Diffraction, and Multispectral Imaging on Mars. *Sci. Adv.* **2022**, *8*, eabp9084. [CrossRef]

171. Taylor, S.R.; McLennan, S. *Planetary Crusts: Their Composition, Origin and Evolution*, 1st ed.; Cambridge University Press: Cambridge, UK, 2010; ISBN 0-521-14201-6.

172. Yen, A.S.; Gellert, R.; Schröder, C.; Morris, R.V.; Bell, J.F.; Knudson, A.T.; Clark, B.C.; Ming, D.W.; Crisp, J.A.; Arvidson, R.E.; et al. An Integrated View of the Chemistry and Mineralogy of Martian Soils. *Nature* **2005**, *436*, 49–54. [CrossRef]

173. Ming, D.W.; Gellert, R.; Morris, R.V.; Arvidson, R.E.; Brückner, J.; Clark, B.C.; Cohen, B.A.; d'Uston, C.; Economou, T.; Fleischer, I.; et al. Geochemical Properties of Rocks and Soils in Gusev Crater, Mars: Results of the Alpha Particle X-ray Spectrometer from Cumberland Ridge to Home Plate. *J. Geophys. Res.* **2008**, *113*, 28. [CrossRef]

174. Gellert, R. *MER APXS Derived Oxide Data Bundle*; NASA: Washington, DC, USA, 2004.

175. Van Bommel, S.J. *MER APXS Derived Oxide Data Bundle*; NASA: Washington, DC, USA, 2020.

176. Gellert, R. *MSL MARS Alpha Particle X-ray Spectrometer 4/5 RDR V1.0. NASA Planetary Data System*; NASA: Washington, DC, USA, 2013. [CrossRef]

177. Gellert, R. *MSL APXS Calibrated Data Collection*; NASA: Washington, DC, USA, 2012.

178. Thompson, L.M.; Spray, J.G.; O'Connell-Cooper, C.; Berger, J.A.; Yen, A.; Gellert, R.; Boyd, N.; McCraig, M.A.; VanBommel, S.J. Alteration at the Base of the Siccar Point Unconformity and Further Evidence for an Alkaline Provenance at Gale Crater: Exploration of the Mount Sharp Group, Greenheugh Pediment Cap Rock Contact With APXS. *J. Geophys. Res. Planets* **2022**, *127*, e2021JE007178. [CrossRef]

179. Goetz, W.; Bertelsen, P.; Binau, C.S.; Gunnlaugsson, H.P.; Hviid, S.F.; Kinch, K.M.; Madsen, D.E.; Madsen, M.B.; Olsen, M.; Gellert, R.; et al. Indication of Drier Periods on Mars from the Chemistry and Mineralogy of Atmospheric Dust. *Nature* **2005**, *436*, 62–65. [CrossRef]

180. Schmidt, M.E.; Perrett, G.M.; Bray, S.L.; Bradley, N.J.; Lee, R.E.; Berger, J.A.; Campbell, J.L.; Ly, C.; Squyres, S.W.; Tesselaar, D. Dusty Rocks in Gale Crater: Assessing Areal Coverage and Separating Dust and Rock Contributions in APXS Analyses. *J. Geophys. Res. Planets* **2018**, *123*, 1649–1673. [CrossRef]

181. VanBommel, S.J.; Knight, A.L.; Schmidt, M.E.; Yingst, R.A.; Henneke, J.; Klevang, D.; Allwood, A.C.; Hurowitz, J.A.; Tice, M.M.; Cable, M.L.; et al. *Compositional and Volumetric Analyses of Dust on the PIXL Calibration Target*; Lunar and Planetary Institute: Houston, TX, USA, 2024; p. Abstract #1598.

182. Piccoli, P.M.; Candela, P.A. Apatite in Igneous Systems. *Rev. Mineral. Geochem.* **2002**, *48*, 255–292. [CrossRef]

183. Adcock, C.T.; Udry, A.; Hauausrath, E.M.; Tschauauner, O. Craters of the Moon National Monument Basalts as Unshocked Compositional and Weathering Analogs for Martian Rocks and Meteorites. *Am. Mineral.* **2018**, *103*, 502–516. [CrossRef]

184. Dymek, R.F.; Owens, B.E. Petrogenesis of Apatite-Rich Rocks (Nelsonites and Oxide-Apatite Gabbronorites) Associated with Massif Anorthosites. *Econ. Geol.* **2001**, *96*, 797–815. [CrossRef]

185. Ihlen, P.M.; Schiellerup, H.; Gautneb, H.; Skår, Ø. Characterization of Apatite Resources in Norway and Their REE Potential—A Review. *Ore Geol. Rev.* **2014**, *58*, 126–147. [CrossRef]

186. Tollari, N.; Toplis, M.J.; Barnes, S.-J. Predicting Phosphate Saturation in Silicate Magmas: An Experimental Study of the Effects of Melt Composition and Temperature. *Geochim. Cosmochim. Acta* **2006**, *70*, 1518–1536. [CrossRef]

187. Krasnova, N.I.; Petrov, T.G.; Balaganskaya, E.G.; Garcia, D.; Moutte, J.; Zaitsev, A.N.; Wall, F. Introduction to Phoscorites: Occurrence, Composition, Nomenclature and Petrogenesis. In *Phoscorites and Carbonatites from Mantle to Mine: The Key Example of the Kola Alkaline Province*; Wall, F., Zaitsev, A.N., Eds.; Mineralogical Society of Great Britain and Ireland: Middlesex, UK, 2004; ISBN 978-0-903056-22-9.

188. Crews, T.E.; Kitayama, K.; Fownes, J.H.; Riley, R.H.; Herbert, D.A.; Mueller-Dombois, D.; Vitousek, P.M. Changes in Soil Phosphorus Fractions and Ecosystem Dynamics across a Long Chronosequence in Hawaii. *Ecology* **1995**, *76*, 1407–1424. [CrossRef]

189. Vitousek, P.M.; Farrington, H. Nutrient Limitation and Soil Development: Experimental Test of a Biogeochemical Theory. *Biogeochemistry* **1997**, *37*, 63–75. [CrossRef]

190. Wardle, D.A.; Walker, L.R.; Bardgett, R.D. Ecosystem Properties and Forest Decline in Contrasting Long-Term Chronosequences. *Science* **2004**, *305*, 509–513. [CrossRef]

191. Brucker, E.; Spohn, M. Formation of Soil Phosphorus Fractions along a Climate and Vegetation Gradient in the Coastal Cordillera of Chile. *Catena* **2019**, *180*, 203–211. [CrossRef]

192. Roncal-Herrero, T.; Oelkers, E.H. Does Variscite Control Phosphate Availability in Acidic Natural Waters? An Experimental Study of Variscite Dissolution Rates. *Geochim. Cosmochim. Acta* **2011**, *75*, 416–426. [CrossRef]

193. Wilson, S.G.; Dahlgren, R.A.; Margenot, A.J.; Rasmussen, C.; O'Geen, A.T. Expanding the Paradigm: The Influence of Climate and Lithology on Soil Phosphorus. *Geoderma* **2022**, *421*, 115809. [CrossRef]

194. Selmants, P.C.; Hart, S.C. Phosphorus and Soil Development: Does the Walker and Syers Model Apply to Semiarid Ecosystems? *Ecology* **2010**, *91*, 474–484. [CrossRef]

195. Lindsay, W.L. Phosphates. In *Chemical Equilibria in Soils*; Wiley: Hoboken, NJ, USA, 1979; p. 478, ISBN 978-0-471-02704-1.

196. Quinn, R.C.; Chittenden, J.D.; Kounaves, S.P.; Hecht, M.H. The Oxidation-Reduction Potential of Aqueous Soil Solutions at the Mars Phoenix Landing Site. *Geophys. Res. Lett.* **2011**, *38*, L14202. [CrossRef]

197. Bandstra, J.Z.; Brantley, S.L. Data Fitting Techniques with Applications to Mineral Dissolution Kinetics. In *Kinetics of Water-Rock Interaction*; Brantley, S.L., Kubicki, J.D., White, A.F., Eds.; Springer: New York, NY, USA, 2008; pp. 211–257, ISBN 978-0-387-73563-4.

198. Huffman, E.O.; Cate, W.E.; Deming, M.E. Rates and mechanisms of dissolution of some ferric phosphates. *Soil Sci.* **1960**, *90*, 8–15. [CrossRef]

199. Thinnappan, V.; Merrifield, C.M.; Islam, F.S.; Polya, D.A.; Wincott, P.; Wogelius, R.A. A Combined Experimental Study of Vivianite and As (V) Reactivity in the pH Range 2–11. *Arsen. Groundw. South-East Asia Emphas. Cambodia Vietnam* **2008**, *23*, 3187–3204. [CrossRef]

200. Vitarella, D.; Moss, O.; Dorman, D.C. Pulmonary Clearance of Manganese Phosphate, Manganese Sulfate, and Manganese Tetraoxide by CD Rats Following Intratracheal Instillation. *Inhal. Toxicol.* **2000**, *12*, 941–957. [CrossRef]

201. Lindsay, W.L.; Vlek, P.L.G.; Chien, S.H. Phosphate Minerals. In *Minerals in Soil Environments*; Dixon, J.B., Weed, S.B., Eds.; Soil Science Society of America: Madison, WI, USA, 1989; p. 1244.

202. Kwon, K.D.; Kubicki, J.D. Molecular Orbital Theory Study on Surface Complex Structures of Phosphates to Iron Hydroxides: Calculation of Vibrational Frequencies and Adsorption Energies. *Langmuir* **2004**, *20*, 9249–9254. [CrossRef]

203. Rampe, E.B.; Morris, R.V.; Archer, P.D.; Agresti, D.G.; Ming, D.W. Recognizing Sulfate and Phosphate Complexes Chemisorbed onto Nanophase Weathering Products on Mars Using In-Situ and Remote Observationsk. *Am. Mineral.* **2016**, *101*, 678–689. [CrossRef]

204. Li, R.; Wang, J.J.; Zhou, B.; Awasthi, M.K.; Ali, A.; Zhang, Z.; Gaston, L.A.; Lahori, A.H.; Mahar, A. Enhancing Phosphate Adsorption by Mg/Al Layered Double Hydroxide Functionalized Biochar with Different Mg/Al Ratios. *Sci. Total Environ.* **2016**, *559*, 121–129. [CrossRef]

205. Roncal-Herrero, T.; Rodríguez-Blanco, J.D.; Benning, L.G.; Oelkers, E.H. Precipitation of Iron and Aluminum Phosphates Directly from Aqueous Solution as a Function of Temperature from 50 to 200 °C. *Cryst. Growth Des.* **2009**, *9*, 5197–5205. [CrossRef]

206. Hsu, P.H. Crystallization of Iron(III) Phosphate at Room-Temperature. *Soil Sci. Soc. Am. J.* **1982**, *46*, 928–932. [CrossRef]

207. Hsu, P.H. Crystallization of Variscite At Room Temperature. *Soil Sci.* **1982**, *133*, 305–313. [CrossRef]

208. Nriagu, J.O.; Dell, C.I. Diagenetic Formation of Iron Phosphates in Recent Lake Sediments. *Am. Mineral.* **1974**, *59*, 13.

209. Tosca, N.J.; McLennan, S.M.; Lindsley, D.H.; Schoonen, M.A.A. Acid-Sulfate Weathering of Synthetic Martian Basalt: The Acid Fog Model Revisited. *J. Geophys. Res.* **2004**, *109*, E05003. [CrossRef]

210. Golden, D.C.; Stewart, R.B.; Tillman, R.W.; White, R.E. Partially Acidulated Reactive Phosphate Rock (PAPR) Fertilizer and Its Reactions in Soil. *Fertil. Res.* **1991**, *28*, 295–304. [CrossRef]

211. Tang, R.; Hass, M.; Wu, W.; Gulde, S.; Nancollas, G.H. Constant Composition Dissolution of Mixed Phases. II. Selective Dissolution of Calcium Phosphates. *J. Colloid Interface Sci.* **2003**, *260*, 379–384. [CrossRef]

212. Borg, L.; Drake, M.J. A Review of Meteorite Evidence for the Timing of Magmatism and of Surface or Near-Surface Liquid Water on Mars. *J Geophys Res* **2005**, *110*, E12S03. [CrossRef]

213. Boyle, F.W.; Lindsay, W.L. Manganese Phosphate Equilibrium Relationships in Soils1. *Soil Sci. Soc. Am. J.* **1986**, *50*, 588–593. [CrossRef]

214. Taylor, S.R.; McLennan, S.M. *Planetary Crusts: Their Composition, Origin, and Evolution*; Cambridge University Press: New York, NY, USA, 2009.

215. Turekian, K.K.; Wedepohl, K.H. Distribution of the Elements in Some Major Units of the Earth's Crust. *GSA Bull.* **1961**, *72*, 175–192. [CrossRef]

216. Fisher, D.J. Pegmatite Phosphates and Their Problems. *Am. Mineral.* **1958**, *43*, 27.

217. Dill, H.G.; Melcher, F.; Gerdes, A.; Weber, B. The Origin and Zoning of Hypogene and Supergene Fe-Mn-Mg-Sc-U-REE Phosphate Mineralization from the Newly Discovered Trutzhofmuhle Aplite, Hagendorf Pegmatite Province, Germany. *Can Miner.* **2008**, *46*, 1131–1157. [CrossRef]

218. Hawthorne, F.C. Structure and Chemistry of Phosphate Minerals. *Miner. Mag* **1998**, *62*, 141–164. [CrossRef]

219. Moore, P.B. Pegmatite Phosphates: Descriptive Mineralogy and Crystal Chemistry. *Mineral. Rec.* **1973**, *4*, 28.

220. Hays, L.E.; Graham, H.V.; Des Marais, D.J.; Hausrath, E.M.; Horgan, B.; McCollom, T.M.; Parenteau, M.N.; Potter-McIntyre, S.L.; Williams, A.J.; Lynch, K.L. Biosignature Preservation and Detection in Mars Analog Environments. *Astrobiology* **2017**, *17*, 363–400. [CrossRef]

221. Hoehler, T.M. An Energy Balance Concept for Habitability. *Astrobiology* **2007**, *7*, 824–838. [CrossRef]

222. Reeves, J.P.; Dowben, R.M. Formation and Properties of Thin-walled Phospholipid Vesicles. *J. Cell. Physiol.* **1969**, *73*, 49–60. [CrossRef]

223. Deamer, D.W.; Oro, J. Role of Lipids in Prebiotic Structures. *Biosystems* **1980**, *12*, 167–175. [CrossRef]

224. Hargreaves, W.R.; Mulvihill, S.J.; Deamer, D.W. Synthesis of Phospholipids and Membranes in Prebiotic Conditions. *Nature* **1977**, *266*, 78–80. [CrossRef]

225. Gulick, A. Phosphorus as a Factor in the Origin of Life. *Am. Sci.* **1955**, *43*, 479–489.

226. Pasek, M.; Lauretta, D. Extraterrestrial Flux of Potentially Prebiotic C, N, and P to the Early Earth. *Orig. Life Evol. Biosph.* **2008**, *38*, 5–21. [CrossRef]

227. Pasek, M.; Block, K. Lightning-Induced Reduction of Phosphorus Oxidation State. *Nat. Geosci* **2009**, *2*, 553–556. [CrossRef]

228. Ritson, D.J.; Mojzsis, S.J.; Sutherland, J.D. Supply of Phosphate to Early Earth by Photogeochemistry after Meteoritic Weathering. *Nat. Geosci.* **2020**, *13*, 344–348. [CrossRef]

229. Toner, J.D.; Catling, D.C. A Carbonate-Rich Lake Solution to the Phosphate Problem of the Origin of Life. *Proc. Natl. Acad. Sci. USA* **2020**, *117*, 883–888. [CrossRef]

230. McGill, W.B.; Cole, C.V. Comparative Aspects of Cycling of Organic C, N, S and P through Soil Organic Matter. *Geoderma* **1981**, *26*, 267–286. [CrossRef]

231. Illmer, P.; Schinner, F. Solubilization of Inorganic Phosphates by Microorganisms Isolated from Forest Soils. *Soil Biol. Biochem.* **1992**, *24*, 389–395. [CrossRef]

232. Jones, D.L.; Oburger, E. Solubilization of Phosphorus by Soil Microorganisms. In *Phosphorus in Action: Biological Processes in Soil Phosphorus Cycling*; Bünemann, E., Oberson, A., Frossard, E., Eds.; Soil Biology; Springer: Berlin/Heidelberg, Germany, 2011; pp. 169–198, ISBN 978-3-642-15271-9.

233. Rogers, J.R.; Bennett, P.C. Mineral Stimulation of Subsurface Microorganisms: Release of Limiting Nutrients from Silicates. *Chem. Geol.* **2004**, *203*, 91–108. [CrossRef]

234. Gyaneshwar, P.; Naresh Kumar, G.; Parekh, L.J.; Poole, P.S. Role of Soil Microorganisms in Improving P Nutrition of Plants. *Plant Soil* **2002**, *245*, 83–93. [CrossRef]

235. Kucey, R.M.N.; Janzen, H.H.; Leggett, M.E. Microbially Mediated Increases in Plant-Available Phosphorus. In *Advances in Agronomy*; Brady, N.C., Ed.; Academic Press: Cambridge, MA, USA, 1989; Volume 42, pp. 199–228.

236. Oburger, E.; Jones, D.L.; Wenzel, W.W. Phosphorus Saturation and pH Differentially Regulate the Efficiency of Organic Acid Anion-Mediated P Solubilization Mechanisms in Soil. *Plant Soil* **2011**, *341*, 363–382. [CrossRef]

237. Banfield, J.F.; Barker, W.W.; Welch, S.A.; Taunton, A. Biological Impact on Mineral Dissolution: Application of the Lichen Model to Understanding Mineral Weathering in the Rhizosphere. *Proc. Natl. Acad. Sci. USA* **1999**, *96*, 3404–3411. [CrossRef]

238. Schaperdoth, I.; Liermann, L.J.; Brantley, S.L. The Effect of Polymeric Substances on Apatite Reactivity in the Presence of a Freshwater Cyanobacterium. *Geomicrobiol. J.* **2007**, *24*, 79–91. [CrossRef]

239. Hausrath, E.M.; Neaman, A.; Brantley, S.L. Elemental Release Rates from Dissolving Basalt and Granite with and without Organic Ligands. *Am. J. Sci.* **2009**, *309*, 633–660. [CrossRef]

240. Neaman, A.; Chorover, J.; Brantley, S.L. Effects of Organic Ligands on Granite Dissolution in Batch Experiments at pH 6. *Am. J. Sci.* **2006**, *306*, 451–473. [CrossRef]

241. Neaman, A.; Chorover, J.; Brantley, S.L. Implications of the Evolution of Organic Acid Moieties for Basalt Weathering over Geological Time. *Am. J. Sci.* **2005**, *305*, 147–185. [CrossRef]

242. Goyne, K.W.; Brantley, S.L.; Chorover, J. Rare Earth Element Release from Phosphate Minerals in the Presence of Organic Acids. *Chem. Geol.* **2010**, *278*, 1–14. [CrossRef]

243. Goyne, K.W.; Brantley, S.L.; Chorover, J. Effects of Organic Acids and Dissolved Oxygen on Apatite and Chalcopyrite Dissolution: Implications for Using Elements as Organomarkers and Oxymarkers. *Chem. Geol.* **2006**, *234*, 28–45. [CrossRef]

244. Tanaka, H.; Miyajima, K.; Nakagaki, M.; Shimabayashi, S. Interactions of Aspartic Acid, Alanie, and Lysine with Hydroxyapatite. *Chem. Pharm. Bull.* **1989**, *37*, 2897–2901. [CrossRef]

245. Hsu, J.; Fox, J.L.; Powell, G.L.; Otsuka, M.; Higuchi, W.I.; Yu, D.; Wong, J.; LeGeros, R.Z. Quantitative Relationship between Carbonated Apatite Metastable Equilibrium Solubility and Dissolution Kinetics. *J. Colloid Interface Sci.* **1994**, *168*, 356–372. [CrossRef]

246. Welch, S.A.; Taunton, A.E.; Banfield, J.F. Effect of Microorganisms and Microbial Metabolites on Apatite Dissolution. *Geomicrobiol. J.* **2002**, *19*, 343–367. [CrossRef]

247. Wei, W.; Zhang, X.; Cui, J.; Wei, Z. Interaction between Low Molecular Weight Organic Acids and Hydroxyapatite with Different Degrees of Crystallinity. *Colloids Surf. Physicochem. Eng. Asp.* **2011**, *392*, 67–75. [CrossRef]

248. Bartlett, C.L.; Hausrath, E.M.; Adcock, C.T.; Huang, S.; Harrold, Z.R.; Udry, A. Effects of Organic Compounds on Dissolution of the Phosphate Minerals Chlorapatite, Whitlockite, Merrillite, and Fluorapatite: Implications for Interpreting Past Signatures of Organic Compounds in Rocks, Soils and Sediments. *Astrobiology* **2018**, *18*, 1543–1558. [CrossRef]

249. Driese, S.G.; Jirsa, M.A.; Ren, M.; Brantley, S.L.; Sheldon, N.D.; Parker, D.; Schmitz, M. Neoarchean Paleoweathering of Tonalite and Metabasalt: Implications for Reconstructions of 2.69Ga Early Terrestrial Ecosystems and Paleoatmospheric Chemistry. *Precambrian Res.* **2011**, *189*, 1–17. [CrossRef]

250. Hausrath, E.M.; Navarre-Sitchler, A.K.; Sak, P.B.; Williams, J.Z.; Brantley, S.L. Soil Profiles as Indicators of Mineral Weathering Rates and Organic Interactions for a Pennsylvania Diabase. *Chem. Geol.* **2011**, *290*, 89–100. [CrossRef]

251. Medaris, L.G.; Driese, S.G.; Stinchcomb, G.E. The Paleoproterozoic Baraboo Paleosol Revisited: Quantifying Mass Fluxes of Weathering and Metasomatism, Chemical Climofunctions, and Atmospheric pCO2 in a Chemically Heterogeneous Protolith. *Precambrian Res.* **2017**, *301*, 179–194. [CrossRef]

252. Brantley, S.L.; Lebedeva, M.; Hausrath, E.M. A Geobiological View of Weathering and Erosion. In *Fundamentals of Geobiology*; Blackwell Publishing Ltd.: Oxford, UK, 2012; pp. 205–227, ISBN 978-1-118-28087-4.

253. Banfield, J.F.; Moreau, J.W.; Chan, C.S.; Welch, S.A.; Little, B. Mineralogical Biosignatures and the Search for Life on Mars. *Astrobiology* **2001**, *1*, 447–465. [CrossRef]

254. Benzerara, K.; Menguy, N. Looking for Traces of Life in Minerals. *Comptes Rendus Palevol* **2009**, *8*, 617–628. [CrossRef]

255. Beveridge, T.J. Role of Cellular Design in Bacterial Metal Accumulation and Mineralization. *Annu. Rev. Microbiol.* **1989**, *43*, 147–171. [CrossRef]

256. Brock, J.; Schulz-Vogt, H.N. Sulfide Induces Phosphate Release from Polyphosphate in Cultures of a Marine Beggiatoa Strain. *ISME J.* **2011**, *5*, 497–506. [CrossRef]

257. Goldhammer, T.; Brüchert, V.; Ferdelman, T.G.; Zabel, M. Microbial Sequestration of Phosphorus in Anoxic Upwelling Sediments. *Nat. Geosci.* **2010**, *3*, 557–561. [CrossRef]

258. Schulz, H.N.; Schulz, H.D. Large Sulfur Bacteria and the Formation of Phosphorite. *Science* **2005**, *307*, 416–418. [CrossRef]

259. Cosmidis, J.; Benzerara, K.; Morin, G.; Busigny, V.; Lebeau, O.; Jézéquel, D.; Noël, V.; Dublet, G.; Othmane, G. Biomineralization of Iron-Phosphates in the Water Column of Lake Pavin (Massif Central, France). *Geochim. Cosmochim. Acta* **2014**, *126*, 78–96. [CrossRef]

260. Konhauser, K.O.; Fyfe, W.S.; Schultze-Lam, S.; Ferris, F.G.; Beveridge, T.J. Iron Phosphate Precipitation by Epilithic Microbial Biofilms in Arctic Canada. *Can. J. Earth Sci.* **1994**, *31*, 1320–1324. [CrossRef]

261. Bailey, J.V.; Corsetti, F.A.; Greene, S.E.; Crosby, C.H.; Liu, P.; Orphan, V.J. Filamentous Sulfur Bacteria Preserved in Modern and Ancient Phosphatic Sediments: Implications for the Role of Oxygen and Bacteria in Phosphogenesis. *Geobiology* **2013**, *11*, 397–405. [CrossRef]

262. Xiao, S.; Knoll, A.H. Fossil Preservation in the Neoproterozoic Doushantuo Phosphorite Lagerstatte, South China. *Lethaia* **1999**, *32*, 219–240. [CrossRef]

263. Mojzsis, S.J.; Arrhenius, G.; McKeegan, K.D.; Harrison, T.M.; Nutman, A.P.; Friend, C.R.L. Evidence for Life on Earth before 3800 Million Years Ago. *Nature* **1996**, *384*, 55–59. [CrossRef]

264. Wacey, D.; Saunders, M.; Roberts, M.; Menon, S.; Green, L.; Kong, C.; Culwick, T.; Strother, P.; Brasier, M.D. Enhanced Cellular Preservation by Clay Minerals in 1 Billion-Year-Old Lakes. *Sci. Rep.* **2014**, *4*, 5841. [CrossRef]

265. Steiner, M.H.; Hausrath, E.H.; Sun, H.J. Synthesis of Potential Phosphate Mineral Biosignatures Under Mars Relevant Conditions. In Proceedings of the 44th Annual Lunar and Planetary Science Conference, Woodlands, TX, USA, 18–22 March 2013; Volume 44, p. 2761.

266. Yang, H.; Sun, H.J.; Downs, R.T. Hazenite, $KNaMg_2(PO_4)2·14H_2O$, a New Biologically Related Phosphate Mineral, from Mono Lake, California, U.S.A. *Am. Mineral.* **2011**, *96*, 675–681. [CrossRef]

267. Yang, H.; Sun, H.J. Crystal Structure of a New Phosphate Compound, Mg2KNa(PO4)2·14H2O. *J. Solid State Chem.* **2004**, *177*, 2991–2997. [CrossRef]

268. Boskey, A.; Spevak, L.; Tan, M.; Doty, S.B.; Butler, W.T. Dentin Sialoprotein (DSP) Has Limited Effects on In Vitro Apatite Formation and Growth. *Calcif. Tissue Int.* **2000**, *67*, 472–478. [CrossRef]

269. Boskey, A.L.; Spevak, L.; Doty, S.B.; Rosenberg, L. Effects of Bone CS-Proteoglycans, DS-Decorin, and DS-Biglycan on Hydroxyapatite Formation in a Gelatin Gel. *Calcif. Tissue Int.* **1997**, *61*, 298–305. [CrossRef]

270. Boskey, A.L.; Maresca, M.; Ullrich, W.; Doty, S.B.; Butler, W.T.; Prince, C.W. Osteopontin-Hydroxyapatite Interactions in Vitro: Inhibition of Hydroxyapatite Formation and Growth in a Gelatin-Gel. *Bone Miner.* **1993**, *22*, 147–159. [CrossRef]

271. Boskey, A.L.; Maresca, M.; Doty, S.; Sabsay, B.; Veis, A. Concentration-Dependent Effects of Dentin Phosphophoryn in the Regulation of in Vitro Hydroxyapatite Formation and Growth. *Bone Miner.* **1990**, *11*, 55–65. [CrossRef]

272. Boskey, A.L.; Maresca, M.; Appel, J. The Effects of Noncollagenous Matrix Proteins on Hydroxyapatite Formation and Proliferation in a Collagen Gel System. *Connect. Tissue Res.* **1989**, *21*, 171–178. [CrossRef]

273. Boskey, A.L. Osteopontin and Related Phosphorylated Sialoproteins: Effects on Mineralization. *Ann. N. Y. Acad. Sci.* **1995**, *760*, 249–256. [CrossRef]

274. Boskey, A.L. Hydroxyapatite Formation in a Dynamic Collagen Gel System: Effects of Type I Collagen, Lipids, and Proteoglycans. *J. Phys. Chem.* **1989**, *93*, 1628–1633. [CrossRef]

275. Bouropoulos, N.; Moradian-Oldak, J. Induction of Apatite by the Cooperative Effect of Amelogenin and the 32-kDa Enamelin. *J. Dent. Res.* **2004**, *83*, 278–282. [CrossRef]

276. Hunter, G.; Hauschka, P.; Poole, A.; Rosenberg, L.; Goldberg, H. Nucleation and Inhibition of Hydroxyapatite Formation by Mineralized Tissue Proteins. *Biochem. J.* **1996**, *317*, 59–64. [CrossRef]

277. Hunter, G.K.; Curtis, H.A.; Grynpas, M.D.; Simmer, J.P.; Fincham, A.G. Effects of Recombinant Amelogenin on Hydroxyapatite Formation In Vitro. *Calcif. Tissue Int.* **1999**, *65*, 226–231. [CrossRef]

278. Hunter, G.K.; Kyle, C.L.; Goldberg, H.A. Modulation of Crystal Formation by Bone Phosphoproteins: Structural Specificity of the Osteopontin-Mediated Inhibition of Hydroxyapatite Formation. *Biochem. J.* **1994**, *300*, 723–728. [CrossRef]

279. Hunter, G.K.; Goldberg, H.A. Nucleation of Hydroxyapatite by Bone Sialoprotein. *Proc. Natl. Acad. Sci. USA* **1993**, *90*, 8562–8565. [CrossRef]

280. Iijima, M.; Moriwaki, Y.; Wen, H.B.; Fincham, A.G.; Moradian-Oldak, J. Elongated Growth of Octacalcium Phosphate Crystals in Recombinant Amelogenin Gels under Controlled Ionic Flow. *J. Dent. Res.* **2002**, *81*, 69–73. [CrossRef]

281. Taira, T.; Iijima, M.; Moriwaki, Y.; Kuboki, Y. A New Method for in Vitro Calcification Using Acrylamide Gel and Bovine Serum. *Connect. Tissue Res.* **1995**, *33*, 185–192. [CrossRef]

282. Tartaix, P.H.; Doulaverakis, M.; George, A.; Fisher, L.W.; Butler, W.T.; Qin, C.; Salih, E.; Tan, M.; Fujimoto, Y.; Spevak, L.; et al. In Vitro Effects of Dentin Matrix Protein-1 on Hydroxyapatite Formation Provide Insights into in Vivo Functions. *J. Biol. Chem.* **2004**, *279*, 18115–18120. [CrossRef]

283. Tye, C.E.; Rattray, K.R.; Warner, K.J.; Gordon, J.A.R.; Sodek, J.; Hunter, G.K.; Goldberg, H.A. Delineation of the Hydroxyapatite-Nucleating Domains of Bone Sialoprotein. *J. Biol. Chem.* **2003**, *278*, 7949–7955. [CrossRef]

284. Wen, H.B.; Moradian-Oldak, J.; Fincham, A.G. Dose-Dependent Modulation of Octacalcium Phosphate Crystal Habit by Amelogenins. *J. Dent. Res.* **2000**, *79*, 1902–1906. [CrossRef]

285. Freche, M.; Lacout, J. LEffect of Humic Compounds and Some Organic Acids Added during Dicalcium Phosphate Dihydrate Crystal Growth Process. *J. Alloys Compd.* **1992**, *188*, 65–68. [CrossRef]

286. Grossl, P.R.; Inskeep, W.P. Kinetics of Octacalcium Crystal Growth in the Presence of Organic Acids. *Geochim. Cosmochim. Acta* **1992**, *56*, 1955–1961. [CrossRef]

287. Van Der Houwen, J.A.M.; Valsami-Jones, E. The Application of Calcium Phosphate Precipitation Chemistry to Phosphorus Recovery: The Influence of Organic Ligands. *Environ. Technol.* **2001**, *22*, 1325–1335. [CrossRef]

288. Blake, R.E. Experimental Investigations of Organic and Microbially Mediated Reactions of Aluminosilicates and Phosphates. Ph.D. Thesis, University of Michigan, Ann Arbor, MI, USA, 1997.

289. Blake, R.E.; O'Neil, J.R.; Surkov, A.V. Biogeochemical Cycling of Phosphorus: Insights from Oxygen Isotope Effects of Phosphoenzymes. *Am. J. Sci.* **2005**, *305*, 596–620. [CrossRef]

290. Chang, S.J.; Blake, R.E. Oxygen Isotope Studies of Phosphite Oxidation: Purification and Analysis of Reactants and Products by High-temperature Conversion Elemental Analyzer/Isotope Ratio Mass Spectrometry. *Rapid Commun. Mass Spectrom.* **2015**, *29*, 2039–2044. [CrossRef]

291. Colman, A.S.; Blake, R.E.; Karl, D.M.; Fogel, M.L.; Turekian, K.K. Marine Phosphate Oxygen Isotopes and Organic Matter Remineralization in the Oceans. *Proc. Natl. Acad. Sci. USA* **2005**, *102*, 13023–13028. [CrossRef]

292. Colman, A.S.; Blake, R.E.; Anna, M.; FOGEL, M.L. 18O of PO4 as a Hydrogeologic Tracer for Nutrient Contamination and Subsurface Microbial Acticity.; 2002.

293. Jaisi, D.P.; Blake, R.E.; Liang, Y.; Chang, S.J. Investigation of Compound-Specific Organic-Inorganic Phosphorus Transformation Using Stable Isotope Ratios in Phosphate. In *Applied Manure and Nutrient Chemistry for Sustainable Agriculture and Environment*; Springer: Berlin/Heidelberg, Germany, 2014; pp. 267–292.

294. Jaisi, D.P.; Blake, R.E. Advances in Using Oxygen Isotope Ratios of Phosphate to Understand Phosphorus Cycling in the Environment. In *Advances in Agronomy*; Elsevier: Amsterdam, The Netherlands, 2014; Volume 125, pp. 1–53, ISBN 0065-2113.

295. Li, H.; Yu, C.; Wang, F.; Chang, S.J.; Yao, J.; Blake, R.E. Probing the Metabolic Water Contribution to Intracellular Water Using Oxygen Isotope Ratios of PO4. *Proc. Natl. Acad. Sci. USA* **2016**, *113*, 5862–5867. [CrossRef]

296. Liang, Y.; Blake, R.E. Oxygen Isotope Fractionation between Apatite and Aqueous-Phase Phosphate: 20–45 C. *Chem. Geol.* **2007**, *238*, 121–133. [CrossRef]

297. Liang, Y.; Blake, R.E. Oxygen Isotope Composition of Phosphate in Organic Compounds: Isotope Effects of Extraction Methods. *Org. Geochem.* **2006**, *37*, 1263–1277. [CrossRef]

298. Liang, Y.; Blake, R.E. Oxygen Isotope Signature of Pi Regeneration from Organic Compounds by Phosphomonoesterases and Photooxidation. *Geochim. Cosmochim. Acta* **2006**, *70*, 3957–3969. [CrossRef]

299. O'Neil, J.R.; Roe, L.J.; Reinhard, E.; Blake, R.E. A Rapid and Precise Method of Oxygen Isotope Analysis of Biogenic Phosphate. *Isr. J. Earth Sci.* **1994**, *43*, 203–212.

300. Sandy, E.H.; Blake, R.E.; Chang, S.J.; Jun, Y.; Yu, C. Oxygen Isotope Signature of UV Degradation of Glyphosate and Phosphonoacetate: Tracing Sources and Cycling of Phosphonates. *J. Hazard. Mater.* **2013**, *260*, 947–954. [CrossRef]

301. Blake, R.E.; Alt, J.C.; Martini, A.M. Oxygen Isotope Ratios of PO_4: An Inorganic Indicator of Enzymatic Activity and P Metabolism and a New Biomarker in the Search for Life. *Proc. Natl. Acad. Sci. USA* **2001**, *98*, 2148–2153. [CrossRef]

302. Jaisi, D.P.; Kukkadapu, R.K.; Stout, L.M.; Varga, T.; Blake, R.E. Biotic and Abiotic Pathways of Phosphorus Cycling in Minerals and Sediments: Insights from Oxygen Isotope Ratios in Phosphate. *Environ. Sci. Technol.* **2011**, *45*, 6254–6261. [CrossRef]

303. Jaisi, D.P.; Blake, R.E.; Kukkadapu, R.K. Fractionation of Oxygen Isotopes in Phosphate during Its Interactions with Iron Oxides. *Geochim. Cosmochim. Acta* **2010**, *74*, 1309–1319. [CrossRef]

304. Jaisi, D.P.; Blake, R.E. Tracing Sources and Cycling of Phosphorus in Peru Margin Sediments Using Oxygen Isotopes in Authigenic and Detrital Phosphates. *Geochim. Cosmochim. Acta* **2010**, *74*, 3199–3212. [CrossRef]

305. Siebers, N.; Bauke, S.L.; Tamburini, F.; Amelung, W. Short-Term Impacts of Forest Clear-Cut on P Accessibility in Soil Microaggregates: An Oxygen Isotope Study. *Geoderma* **2018**, *315*, 59–64. [CrossRef]

306. Tamburini, F.; Pfahler, V.; von Sperber, C.; Frossard, E.; Bernasconi, S.M. Oxygen Isotopes for Unraveling Phosphorus Transformations in the Soil–Plant System: A Review. *Soil Sci. Soc. Am. J.* **2014**, *78*, 38–46. [CrossRef]

307. Hausrath, E.M.; Martinez, E.; Blake, R.E.; Udry, A.; McCubbin, F.M.; Wostbrock, J.; Hayles, J. Examining the Oxygen Isotope Composition of Phosphate as a Potential Biosignature in Returned Martian Samples. In Proceedings of the 2024 Astrobiology Science Conference, Providence, RI, USA, 5–10 May 2024; p. Abstract 211-04.